Thermodynamic properties of minerals and fluids

Alekhin Yu.V., Fiaizullina R.V., Bychkov D.A. Reality of formation of Hg_2O solution in liquid mercury and mercury gashydrate according to topological analysis data by the Skrainemakers method

M.V. Lomonosov Moscow State University, Department of Geology, Moscow alekhin@geol.msu.ru ; fiaizullina@geol.msu.ru ; krok@geol.msu.ru

Abstract. Using the results of numerous experiments on the «solubility of liquid mercury» in water, Skreinemakers's topological analysis of the composition of the aqueous phase with respect to valence forms of mercury showed that liquid mercury in the Hg-H_2O system is a solution of Hg_2O in Hg(liq.). This is determined by the dominance of the $Hg_2(OH)_2^0$ complex in the composition of the equilibrium aqueous phase. Calculations using the Gibbs-Duhem equation show that the fraction of the Hg_2O minal in the liquid mercury solution is large, with the minimum of HgO minal content. A more detailed analysis of the system for the solubility of valence forms of mercury showed that at low temperatures and the standard volatility of oxygen in aqueous solutions, the $Hg(OH)_2^0$ form is dominant in equilibrium with Hg(liq.), and the mercury (I) complex is dominated by $Hg_2(OH)_2^0$, and in the liquid aqueous phase the concentration of mercury is ensured by its solubility. This explains why the saturation concentration in the Hg(liq.) phase is two orders of magnitude lower than the solubility of montrodite (HgO).

Keywords: *mercury; mercury gashydrate; Skreinemakers's topological analysis; solubility of liquid mercury; mercury valence forms.*

The valent states of mercury are known: Hg (0), Hg (I) and Hg (II), whose dominance in natural conditions is determined precisely by oxidation-reduction conditions. Therefore, the choice of the volatility of oxygen as determining the intensive parameter, along with the temperature, in the analysis of phase relationships was inevitable. The review includes 6 phases: L_1 - liquid mercury phase, L_2 - liquid water phase, G - gas, I - ice of water, S_0 - solid elemental mercury and S_1 - Hg (II) oxide, montroidite, phase of stoichiometric composition HgO, stable at unrealistically high $f\,O_2$. The mercury hemioxide Hg (I) of Hg_2O (S_2) composition, the nature of its non-autonomy, the nature of the thermodynamic instability of the solid phase $Hg(OH)_2$ is considered. It was not necessary to resort to methods of complete topological analysis when analyzing the stability it is sufficient to use an augmented base of thermochemical quantities (table) and known equilibrium constants of mercury forms. Therefore, the analysis of a multi-system of 6 phases was similar to a detailed study of the H_2O-CO_2 system (Alekhin, Zakirov 1971, Alekhin et al., 1973), but with one radical difference: in the H_2O-CO_2 system, the phase equilibria were analyzed in *P-T* coordinates, reasons to study the shape of the components at $f\,O_2$ in other valence states, including, elemental carbon, CO, CH_4, hydrocarbons. The concrete problem of stability of the $CO_2 \cdot 5¾\ H_2O$ clathrate was solved, i.e. carbon dioxide gas hydrate, which for the first time in world practice made it possible to show the inevitability of the formation and stability of this ice phase on the polar caps of Mars. The return to this approach is caused by loud publications (Schuster et al., 2018) on the mercury content in permafrost, in the ice cover of the Earth, in the absence of good versions about the nature of these inputs, the phase forms of binding (immobilization) and the reality of secondary emissions.

A new problem is the approach to the problem of the instability of the gas hydrate $Hg \cdot 6H_2O$, that is, the clathrate compound of mercury. At a preliminary stage, it is difficult to choose between this gas hydrate and the $Hg_2O \cdot 6H_2O$ clathrate at close enthalpy values of formation by the rules of supramolecular chemistry (Len, 1998) and small values of the enthalpy of the decay of clathrates.

For the Hg – H_2O multi-system, the key task was to analyze the phase compositions, as well as the dominant dissolved complexes, under the univariant L_1L_2G equilibrium (Figure), where both liquid phases change composition with changing fO_2 and temperature. In water, the main forms are Hg (aq.) neutral hydroxocomplexes $Hg_2(OH)_2^0$ and $Hg(OH)_2^0$ with the dominance of the first complex - Hg (I). The presence in the aqueous phase of all three valence states at atmospheric $f\ O_2 = 0.208$ and the well-studied tendency of mercury mineral phases to form structures with the covalent pair -Hg-Hg-, and the minerals HgO and Hg_2O- to have a high affinity for Hg (liq.), makes L_1 as a dilute solution in Hg (0) of these minals. We develop this version for the first time, but the absence of any experimental and structural data on the composition of the L_1 phase forces both topological analysis and the solution of the Gibbs-Duhem equation for the coexisting L_1L_2 liquid phases with varying oxygen fugacity. The equilibrium ends at a non-invariant point with parameters very close to the triple point of water (T = -0.01 °C and log P = -2.236) for IL_1L_2G, and the stability of the three aqueous phases with liquid mercury is beyond doubt (Figure 1). The second is the same non-invariant point: S_0IL_1G, is an analog of the triple point for mercury with well-known tabulated *P-T* parameters (T = -38.8344 °C, lg P_{atm} = -9.25664) plus ice water. These two invariant points are interconnected by a completely stable univariant equilibrium where simultaneous sublimation of two solid phases occurs: $I + S_0 \rightarrow G$ up to the lowest temperatures and oxygen fugitives with rapidly decreasing vapor pressures over these solid phases.

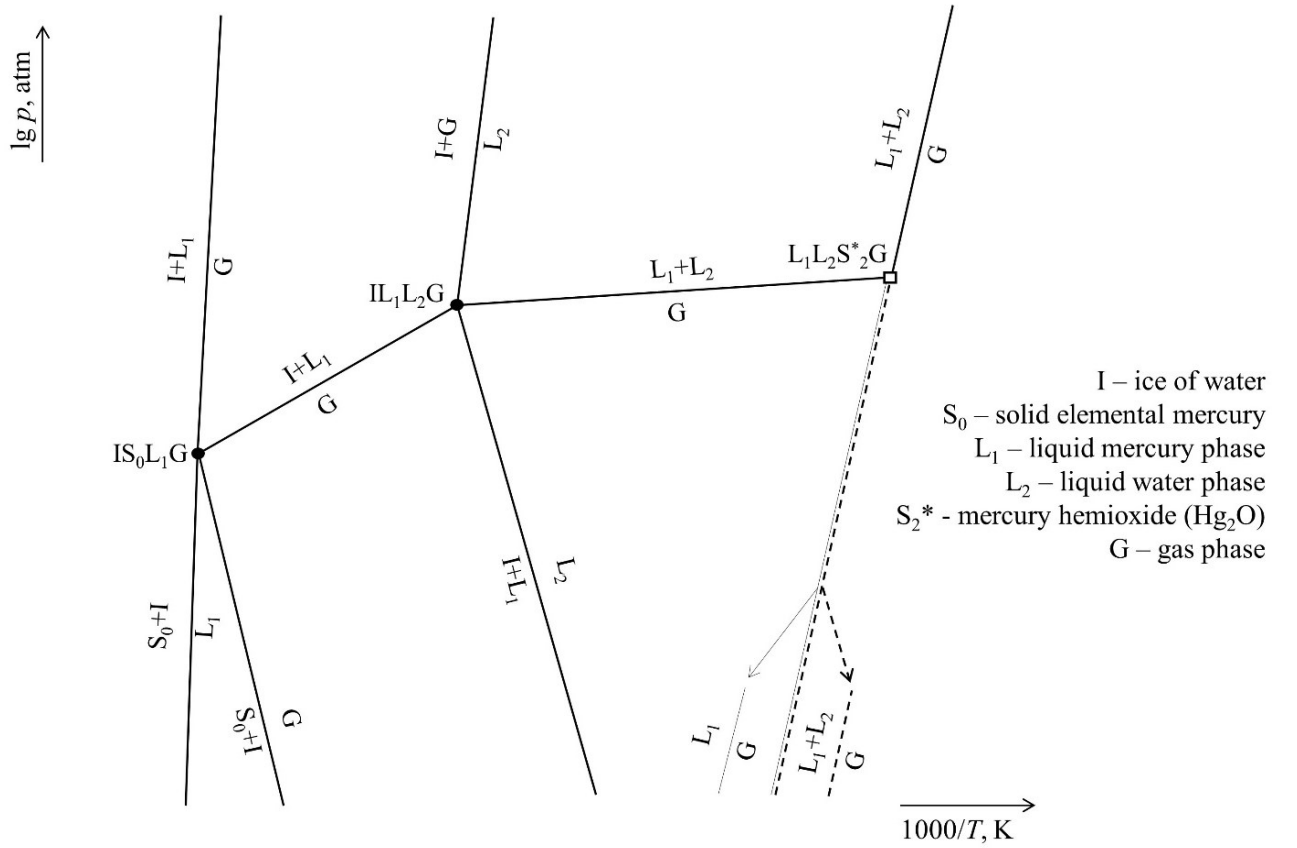

Figure. Topological scheme for the system Hg – H_2O

Using the data of standard production energies, the molality ratio of the three dominant valence forms is calculated: Hg^0(p-p), $Hg_2(OH)_2^0$ and $Hg(OH)_2^0$ at a well-known, repeatedly studied value of gross solubility (lg mΣ). This calculation, using the standard values of the free energy of formation, must be carried out according to the reaction:

$$2H_2O+O_2 + 2Hg_2(OH)_2^0 \rightleftarrows 4Hg(OH)_2^0,$$

but with considering the volatility of O_2 (0.5 lg fO_2 = -0.341). In this case, the molar quantities of the forms are equal to lg m (Hg^0 (aq.)) = -8.01 (Alekhin et al., 2011); lg $m(Hg(OH)_2^0)$ = -8.351 and lg $2m(Hg_2(OH)_2^0)$ = -6.518.

All the results of topological analysis (Skreinemakers, 1948) are based on the thermochemical data of particles and phases in a consistent system of values (Table) for the state of both an ideal infinitely dilute solution (⊖) and for standardization from a pure edge phase (^{0}), which makes it easy to calculate Henry's constants and standard transition energies, which is important in the presence of non-autonomous phases (Prigogine, Defay, 1966).

All the valence forms distributed in natural waters differ in contrast by their solubility and migration mobility. Elemental mercury due to low solubility (Alekhin et al., 2011) (the solubility of elemental mercury in the form of Hg^0 (aq.) at 25°C is 0. $977 \cdot 10^{-8}$ mol/l or 1.96 μ g/l, the total solubility of the sum of three valence forms over liquid mercury is 61.14 μ g/l), that is, the mercury in the form of a neutral hydroxocomplex Hg (I) of $Hg_2(OH)_2^0$ predominates in the aqueous phase, and $Hg(OH)_2^0$ and Hg^0 (aq.). It is believed that in the atmosphere in the gaseous state, the former dominates in the form of Hg^0 vapor, being the main source and the transit form of the appearance of other mobile and deposited forms, which, strictly speaking, has not been proven.
It is believed that the divalent mercury ion is the dominant valence form in natural waters, but this is far from obvious, in particular for the existence of a zero-valent-form emission source, which follows from the analysis of the electrochemical reaction of redox disproportionation:

$$Hg_2^{2+} \rightleftarrows Hg^{2+} + Hg^0(liq.).$$

The positive (but small) value of the standard EMF (0.043B) of this reaction indicates that the Hg^{2+} ions in the presence of an elementary form (for example, liquid mercury) can easily transform into ionic dimers: Hg_2^{2+}. A small value of E^o for liquid mercury in the Nernst equation:

$$E = E^0 + RT \ln\left(\frac{\left[Hg^{2+}\right]\cdot\left[Hg^0(liq.)\right]}{\left[Hg_2^{2+}\right]}\right)$$

and precisely in the presence of liquid mercury, when a (Hg^0) = 1, unambiguously indicates a real possibility of predominance in the waters of any of the other two valence forms: Hg_2^{2+} and Hg^{2+}.

Table. Values of free energies of formation

Phase	$\Delta G°f_{298,15}$, kkal/mol	A source
Hg^0(liq.)	0	
HgO(cr.) hex.	-13,95	TCV (thermal constant values)
HgO(cr.) red	-14,015	on the solubility of phases (>6 μ m)
HgO(cr.) yel.	-13,986	on the solubility of phases (<4 μ m)
Hg_2O^0	-21,5	Karapetyants, 1955
$Hg_2O^{\ominus}$	-13,002	Chem. encyclopedia. Ed. N.S. Zefirov. Vol.4. 1995
$Hg^{\ominus}$ (aq.)	10,9256	Alekhin et al., 2011
$Hg_2(OH)_2^{\ominus}$	-38,488	agreed with (Naumov et al, 1971)
$Hg(OH)_2^{\ominus}$	-65,71	agreed with (Naumov et al, 1971)
$Hg_2(OH)_2$(s.)	-70,6774	agreed with (Naumov et al, 1971)
$Hg_2^{2+\ominus}$	36,70	agreed with (Naumov et al, 1971)
$Hg^{2+\ominus}$	39,30	agreed with (Naumov et al, 1971)
$HgOH^{+\ominus}$	-12,50	agreed with (Naumov et al, 1971)

The shift of equilibrium in the presence of a zero-valent form is easily carried out both in the natural environment and under technogenic influence. This effect is also inevitable for the initial absence of a zero-valence form in the form Hg^0 (aq.). Any shift of equilibrium toward the formation of Hg (II) in the presence of Hg (I) leads to the generation of Hg (0), which either accumulates in the liquid drop phase or enters the atmosphere as a vapor phase. Also, when Hg (II) is bound to well-known chloride complexes, in the presence of liquid mercury, a corresponding decrease in the concentration of the Hg_2^{2+} ion is required when shifting the disproportionation equilibrium to the right with the formation of liquid mercury and the Hg^{2+} ion. In view of the foregoing, when assessing the geochemical situation, it is important to determine not so much the gross composition as the ratio between the different valence forms of mercury that control the fine mechanisms of geochemical migration. Therefore, in the practice of analytical work, it is necessary to have methods that allow calculating the proportions of valence forms, or to determine them. The problem of analytical, (preparative) separation of oxidized forms of mercury from the elementary form is insoluble because of the complete thermodynamic lability of all redox and hydration equilibria. A separate problem of experimental geochemistry in studying the mercury cycle is the question of how much of the elementary mercury vapor in solution and in the gas phase can be hydrated. According to our data, elemental mercury in the form of Hg^0 (aq.) is practically insoluble in water. There is reason to believe that the value of 2 mg/l is somewhat overestimated, but under normal oxidative conditions with oxygen fugacity of 0.208 atm, the saturation of water upon contact with liquid mercury is provided by the hydroxocomplexes of $Hg(OH)_2^0$, and most importantly, $Hg_2(OH)_2^0$ up to 60 mg/l). First, elemental mercury itself, by its own chemical properties, should be close to noble metals, in which the solubility is 1.5-2 orders of magnitude lower, but its proximity to hydrogen in the series of stresses demonstrates the duality of behavior and causes a relatively high ability to oxidize. Secondly, in the high-temperature region, when Hg (0) begins to predominate over the oxidized forms due to their complete thermal dissociation, the lg m – 1/T dependence becomes an extremely simple linear function. And the solubility of mercury near room temperature does not allow this dependence to manifest itself in the same form, that is, the concentrations are overstated compared to the linear law, which is associated with the appearance of already analytically significant amounts of oxidized forms of mercury in comparison with Hg (0). Thirdly, using our data on the solubility of Hg^0 in a reducing environment and tabulated data on vapor pressure over liquid mercury, it is easy to calculate the Henry constant. According to the formula $m = B \cdot p$, we have lg B = 0.7, that is, a value close to the constants for gases such as carbon dioxide and hydrogen sulfide, while it should be close to the constants of inert gases. The Henry's constants, which are close to the constants of strongly hydratable hydrogen sulfide and carbon dioxide, are due to overestimation of the mercury concentration in the solution due to the presence in the seemingly simple equilibrium of water-liquid mercury of the dominant and better soluble mercury forms of other valence states.

Analysis of equilibrium valence forms showed that for the composition of fluid phases, the non-autonomy of the oxide film as a phase on the surface of liquid mercury is key (Prigogine, Defay, 1966). Their simultaneous participation in geochemical processes and mercury cycle demonstrates the migration and distribution of valence forms of mercury in the atmosphere, hydrosphere and lithosphere.

This work was supported by a grant from the Russian Foundation for Basic Research No. 17-05-01055-a.

References:

Alekhin Yu.V., Zakirov I.V. CO_2 5¾H_2O gas hydrate as the most probable solid phase of the polar caps of Mars //

Abstracts at the Congress of the WMO. – Leningrad, 1971. – P. 21. – In Rus.
Alekhin Yu.V., Zharikov V.A., Zakirov I.V. System H_2O – CO_2 and the atmosphere of the planets // The results of science and technology. Geochemistry. Mineralogy. Petrography. – Vol. 7. – Moscow: VINITI, 1973. – P. 5–78. – In Rus/
Alekhin Y.V., Zagrtdenov N.R., Mukhamadiyarova R.V. Hg°(liq.) – Hg°(aq.) equilibrium and solubility of elementary mercury in water // Moscow University Geology Bulletin. – 2011. – Vol. 66. – No. 6. – P. 439–441.
Karapetyants M.H. An approximate method for calculating the isobaric potentials and heats of the formation of various substances // Proceedings of the Moscow Chemical and Technological Institute named after D.I. Mendeleyev, 1955. Is. 20. – P. 10–38. – In Rus.
Len Zh.M. Supramolecular chemistry: Concepts and perspectives. – Novosibirsk: Science, 1998. – 334 p.
Naumov G.B., Ryzhenko B.N., Khodakovskiy I.L. Handbook of thermodynamic quantities (for geologists). – Moscow: Atomizdat. – 240 p. – In Rus.
Prigogine I., Defay R. Chemical Thermodynamics. – Novosibirsk: Science, Sib. Department, 1966. – 512 p. – In Rus.
Skreinemakers F.A. Unvariant, univariant and divariant equilibria. Moscow, 1948. – 215 p. – In Rus.
Schuster P.F., Schaefer K.M. et al. Permafrost Stores a Globally Significant Amount of Mercury // Geophysical Research Letter, 2018. – Vol. 45. – P. 1-9.

Eremin O.V., Epova E.S. The system of increments for calculation of standard Gibbs potentials of uranovanadates minerals.

M.V. Institute of natural resources, ecology and cryology SB RAS, Chita (yeroleg@yandex.ru)

Abstract. On the basis of experimentally determined values of the standard Gibbs energies of formation from elements for uranovanadates of different metals were calculated the oxide increments by using the methods of linear programming. The obtained system of increments was used for estimation the unknown Gibbs energies of uranovanadates minerals.

Keywords: uranovanadates, Gibbs energy, linear programming, oxides increments.

Uranovanadates are one of the most widespread chemical classes of uranium minerals. The minerals of this class registered to date are given in (Table 1).

A number of synthetic uranonadates of various metals have been obtained (Chernorukov et al., 2002, Karyakin et al., 2001, 2003; Suleimanov et al., 2004), for which the standard Gibbs energies of formation from elements are determined. On the basis of these data, in this paper we present a system of increments for estimating the thermodynamic potentials of uranovanadates.

For compounds with known values of standard Gibbs energies, which we call calibrating, we record the reactions of their formation from the constituent oxides:

$$\sum Ox = M, \quad (1)$$

where Ox are the composite oxides of the mineral (compound) M.

For the reactions (1) we formulate the problems of linear programming of the form:

$$\min \mathbf{Gx}, \mathbf{Ax}=\mathbf{b}, \mathbf{x}\geq 0, \quad (2)$$

where **G** is the standard Gibbs energy of formation from the elements of the reaction components (1), **x** is their molar quantities, **A** is the stoichiometric matrix; **Ax** = **b**, **x**≥0 - mass balance conditions in a closed system. The solutions **y*** of problems dual to (2):

$$\mathbf{y}^* = \max \mathbf{by}, \mathbf{A}'\mathbf{y} \leq \mathbf{G}, \quad (3)$$

where ' is the transpose index can be represented in the form of linear expansions of the free energies of reaction products (1) according to the stoichiometric contributions of composite oxides (Eremin et al., 2016):

$$G(M) = \sum k(i) y^*(i), \quad (4)$$

where k (i) are the stoichiometric coefficients of the corresponding y *(i) - potentials of oxide increments i. For example, for the set U-V-O-H and reaction (1):

$3UO_3 + V_2O_5 + 4H_2O = (UO_2)_3(VO_4)_2 \cdot 4H_2O$, the expansion (4) has the form

$$G((UO_2)_3(VO_4)_2 \cdot 4H_2O) = -5899.000 \text{(kJ/mole)} \text{ (Nipruk et al., 2013)} = -1158.329k(UO_3) - 1467.976k(V_2O_5) - 239.009k(H_2O). \quad (5)$$

Table 1. Minerals of uranovanadates class, according to data (Spano et al., 2017; IMA, 2017)

Mineral (formula)	Mineral (formula)
Carnotite $K_2(UO_2)_2(VO_4)_2 \cdot 3H_2O$	Mathesiusite $K_5(UO_2)_4(SO_4)_4(VO_5) \cdot 4H_2O$
Crichtonite $Sr(Mn,Y,U)Fe_2(Ti,Fe,Cr,V)_{18}(O,OH)_{38}$	Metatyuyamunite $Ca(UO_2)_2(VO_4)_2 \cdot 3H_2O$
Curienite $Pb(UO_2)_2(VO_4)_2 \cdot 5H_2O$	Metavanuralite $Al(UO_2)_2(VO_4)_2(OH) \cdot 8H_2O$
Davidite-(Ce) $Ce(Y,U)Fe_2(Ti,Fe,Cr,V)_{18}(O,OH,F)_{38}$	Rauvite $Ca(UO_2)_2V_{10}O_{28} \cdot 16H_2O$
Davidite-(La) $La(Y,U)Fe_2(Ti,Fe,Cr,V)_{18}(O,OH,F)_{38}$	Sengierite $Cu_2(UO_2)_2(VO_4)_2(OH)_2 \cdot 6H_2O$
Dessauite-(Y) $Sr(Y,U,Mn)Fe_2(Ti,Fe,Cr,V)_{18}(O,OH)_{38}$	Strelkinite $Na_2(UO_2)_2(VO_4)_2 \cdot 6H_2O$
Finchite $Sr(UO_2)_2(V_2O_8) \cdot 5H_2O$	Metastrelkinite $Na_2(UO_2)_2(VO_4)_2 \cdot 2H_2O$
Francevillite $Ba(UO_2)_2(VO_4)_2 \cdot 5H_2O$	Tyuyamunite $Ca(UO_2)_2(VO_4)_2 \cdot 5\text{-}8H_2O$
Fritzscheite $Mn(UO_2)_2(VO_4,PO_4)_2 \cdot 4H_2O$	Uvanite $(UO_2)_2V_6O_{17} \cdot 15H_2O$
Margaritasite $Cs_2(UO_2)_2(VO_4)_2 \cdot H_2O$	Vanuralite $Al(UO_2)_2(VO_4)_2(OH) \cdot 11H_2O$

Table 2. The values of standard Gibbs energies of formation from the elements -G (kJ/mol) of compounds used in the calculations of equations (1-4).

Oxides	-G, kJ/mole	Reference	Compounds	-G, kJ/mole	Reference
Na_2O	375.480	(Yokokawa, 1988)	$NaVUO_6{\cdot}2H_2O$	2758.000	(Karyakin et al., 2001)
K_2O	320.700	« »	$KVUO_6$	2289.000	« »
Cs_2O	308.160	« »	$CsVUO_6$	2317.000	« »
CaO	604.048	« »	$Ca(VUO_6)_2{\cdot}5H_2O$	5735.000	(Karyakin et al., 2003)
SrO	561.899	« »	$Sr(VUO_6)_2{\cdot}5H_2O$	5789.000	« »
BaO	525.100	« »	$Ba(VUO_6)_2{\cdot}4H_2O$	5570.000	« »
MnO	362.920	« »	$Mn(VUO_6)_2{\cdot}4H_2O$	5182.000	(Chernorukov et al., 2002)
CuO	129.500	« »	$Cu(VUO_6)_2{\cdot}4H_2O$	4798.000	« »
PbO	188.950	« »	$Pb(VUO_6)_2{\cdot}5H_2O$	5226.000	(Suleimanov et al., 2004)
Al_2O_3	1582.280	« »	$Al(PUO_6)_2(OH){\cdot}11H_2O$	7515.000	(Chernorukov et al., 2002)
UO_3	1142.270	« »	$(UO_2)_3(VO_4)_2{\cdot}4H_2O$	5899.000	(Nipruk et al., 2013)
V_2O_5	1419.602	« »			
H_2O	231.181	« »			

Table 3. The values of oxide increments -y * (kJ / mole) for Me-U-V-O-H system.

	y*(MeOx)	y*(V_2O_5)	y* (H_2O)	y*(UO_3)	Calibrating compounds
Na_2O	460.257	1555.760	270.723	1208.545	$NaVUO_6{\cdot}2H_2O$
K_2O	459.117	1583.053	-	1267.915	$KVUO_6$
Cs_2O	464.365	1599.293	-	1285.170	$CsVUO_6$
CaO	661.179	1498.260	239.652	1188.649	$Ca(VUO_6)_2{\cdot}5H_2O$
SrO	645.406	1534.709	239.641	1205.339	$Sr(VUO_6)_2{\cdot}5H_2O$
BaO	615.639	1550.348	243.160	1215.685	$Ba(VUO_6)_2{\cdot}4H_2O$
MnO	407.269	1477.702	238.691	1171.132	$Mn(VUO_6)_2{\cdot}4H_2O$
CuO	136.955	1423.361	238.268	1142.305	$Cu(VUO_6)_2{\cdot}4H_2O$
PbO	226.676	1464.395	239.243	1169.357	$Pb(VUO_6)_2{\cdot}5H_2O$
Al_2O_3	1701.112	-	261.952	1142.644	$Al(PUO_6)_2(OH){\cdot}11H_2O$

Table 4. Gibbs energies -G (kJ/mole), calculated on the basis of values of oxide increments (Table 3) and decomposition (5).

Mineral (formula)	-G, kJ/mole	Calibrating compounds
Curienite $Pb(UO_2)_2(VO_4)_2{\cdot}5H_2O$	5226.000	$Pb(VUO_6)_2{\cdot}5H_2O$
Finchite $Sr(UO_2)_2(V_2O_8){\cdot}5H_2O$	5789.000	$Sr(VUO_6)_2{\cdot}5H_2O$
Francevillite $Ba(UO_2)_2(VO_4)_2{\cdot}5H_2O$	5813.160	$Ba(VUO_6)_2{\cdot}4H_2O$
Fritzscheite $Mn(UO_2)_2(VO_4,PO_4)_2{\cdot}4H_2O$	5182.000	$Mn(VUO_6)_2{\cdot}4H_2O$
Metatyuyamunite $Ca(UO_2)_2(VO_4)_2{\cdot}3H_2O$	5255.695	$Ca(VUO_6)_2{\cdot}5H2O$
Rauvite $Ca(UO_2)_2V_{10}O_{28}{\cdot}16H_2O$	14364.217	« »
Sengierite $Cu_2(UO_2)_2(VO_4)_2(OH)_2{\cdot}6H_2O$	5649.759	$Cu(VUO_6)_2{\cdot}4H_2O$
Strelkinite $Na_2(UO_2)_2(VO_4)_2{\cdot}6H_2O$	6057.446	$NaVUO_6{\cdot}2H_2O$
Metastrelkinite $Na_2(UO_2)_2(VO_4)_2{\cdot}2H_2O$	4974.554	« »
Tyuyamunite $Ca(UO_2)_2(VO_4)_2{\cdot}5H_2O$	5735.000	$Ca(VUO_6)_2{\cdot}5H2O$
Tyuyamunite $Ca(UO_2)_2(VO_4)_2{\cdot}8H_2O$	6453.957	« »
Uvanite $(UO_2)_2V_6O_{17}{\cdot}15H_2O$	10305.719	$(UO_2)_3(VO_4)_2{\cdot}4H_2O$
Carnotite $K_2(UO_2)_2(VO_4)_2{\cdot}3H_2O$	3022.500	$KVUO_6$+ G(H_2Oкр.)
Margaritasite $Cs_2(UO_2)_2(VO_4)_2{\cdot}H_2O$	2561.500	$CsVUO_6$+ G(H_2Oкр.)
Vanuralite $Al(UO_2)_2(VO_4)_2(OH){\cdot}11H_2O$	7383.792	$(UO_2)_3(VO_4)_2{\cdot}4H_2O$+ y*($Al_2O_3$)
Metavanuralite $Al(UO_2)_2(VO_4)_2(OH){\cdot}8H_2O$	6666.766	$(UO_2)_3(VO_4)_2{\cdot}4H_2O$+ y*($Al_2O_3$)

For Me-U-V-O-H system, the linear expansions (4) are presented in (Table 3).

Using the values of the increments (Table 3) and the expansion (5), the values of the standard Gibbs energies of minerals of the uranovanadate class were calculated (Table 4).

The minerals (Table 4), whose Gibbs energies are represented to an accuracy of .000 (kJ/mol), correspond to the stoichiometric formulas of the synthetic compounds chosen as calibration substances for which the potentials are equal to the sums of the constituent oxide increments, according to equation (4). For the minerals of carnotite and margaritasite, the Gibbs energies are estimated using the following algorithm. From the potential difference $G(NaVUO_6 \cdot 2H_2O)-G(NaVUO_6)$= -2758.000-2269.000=-489.000 (kJ/mole) it is possible to determine the energy of crystal water $G(H_2Ocr.)$=-489.000/2=-244.500(kJ/mol). This value was used in the additive estimation by formulas: $G(carnotite)=G(KVUO_6)+3G(H_2Ocr.)$= -2289.000+3*(-244.500)=-3022.500(kJ/mole); $G(margaritasite)=G(CsVUO_6)+G(H_2Ocr.)$= -2317.000-244.500=-2561.500(kJ/mol).

For minerals of vanuralite and metavanuralite, the increments of equation (5) are used plus $y*(Al_2O_3)$=-1701.112(kJ/mole), obtained by the decomposition (4) for aluminum uranium phosphate (Table 3).

The obtained values of the standard Gibbs potentials are included in the "Selector" PC database for use in geochemical calculations.

References:

Chernorukov N. G., Karyakin N. V., Suleimanov E. V., Barch S. V., Alimzhanov M. I. (2002) Thermodynamics of aluminum uranophosphate and aluminum uranoarsenate. Radiochemistry. 44, 216-218.

Chernorukov N. G., Karyakin N. V., Suleimanov E. V., Knyazev A. V., and Feoktistova O. V. (2002) Thermochemistry of $AII(VUO_6)_2 \cdot nH_2O$ Compounds (AII = Mn, Fe, Co, Ni, Cu, Zn, Cd). Russian Journal of General Chemistry, Vol. 72, No. 2, pp. 178-182.

Eremin O.V., Epova E.S., Rusal O.S., Filenko R.A., Bychinskii V.A., Chudnenko K.V., Fomichev S.V., Krenev V.A. (2016) The unified method for computing thermodynamic properties of natural zeolites based on their crystallochemical formulas. Russian Journal of Inorganic Chemistry, Vol. 61, No. 8, pp. 1003–1012.

IMA, 2017. The new IMA list of minerals – a work in progress. Updated: November 2017. http://nrmima.nrm.se

Karyakin N. V., Chernorukov N. G., Suleimanov E. V., Alimzhanov M. I. (2003) Chemical Thermodynamics of Alkaline-Earth Metal Uranovanadates. Radiochemistry, Vol. 45, No. 5, 2003, pp. 457-468.

Karyakin N. V., Chernorukov N. G., Suleimanov E. V., Alimzhanov M. I. (2001) Thermodynamics of Alkali Metal Uranovanadates. Russian Journal of General Chemistry, Vol. 71, No. 9, pp. 1333-1341.

Nipruk O.V., Chernorukov N.G., Volochai A.A., Arova M.I. (2013)
Study of the state of uranyl orthovanadate $(UO_2)_3(VO_4)_2 \cdot 4H_2O$ in aqueous solutions. Russian Journal of General Chemistry, V. 83. № 4. P. 636-641.

Spano T.L., Dzik E.A., Sharifironizi M., Dustin M.K., Turner M., Burns P.S. (2017) Thermodynamic investigation of uranyl vanadate minerals: Implications for structural stability. American Mineralogist, Vol. 102, pp. 1149–1153.

Suleimanov E. V., Chernorukov N. G., Golubev A. V. (2004) Synthesis, Structure, and Physicochemical Properties of Compounds $Pb(B^VUO_6)_2 \cdot nH_2O$ (B^V = P, As, V). Radiochemistry, Vol. 46, No. 5, pp. 446-451.

Yokokawa H. (1988) Tables of thermodynamic properties of inorganic compounds. Journal of the national chemical laboratory for industry. Tsukuba Ibaraki 305, Japan. 83, 27-118.

Ivanov M.V., Bushmin S.A. Thermodynamic model of the system H_2O-CO_2-$CaCl_2$ at high PT parameters

Institute of Precambrian Geology and Geochronology RAS, Sankt Petersburg (m.v.ivanov@ipgg.ru)

Abstract. The thermodynamic model of the system H_2O-CO_2-$CaCl_2$ for high pressures and temperatures is developed on the basis of an equation for the Gibbs free energy. The equation for the concentration dependence of the excess Gibbs free energy coincides with that suggested by Aranovich et al (2010). Our parameterization of the PT-dependencies of the coefficients of this equation is based on the molar volume of water at corresponding PT values. Our model enables obtaining the phase state (homogeneous or multi-phase) of the fluid, activities of the components, and their concentrations in the coexisting phases. The model reproduces all available experimental data on the phase decomposition in the ternary system H_2O-CO_2-$CaCl_2$ (Zhang, Frantz, 1989; Shmulovich, Graham, 2004). These experimental data cover the range of temperatures and pressures 500-800°C and 1-9 kb correspondingly. The natural parameterization of the PT-dependencies introduced in our model allows us to assume the model to be valid beyond the boundaries of the experimentally studied area.

***Keywords**: high temperature, high pressure, fluid, phase decomposition, CO_2, $CaCl_2$*

Calcium chloride, along with the most common NaCl, is the most important salt of natural water-salt fluids. Fluids rich in $CaCl_2$, including those containing carbon dioxide, play an important role in the deep processes of metamorphism and metasomatism, the transport of deep ore matter into the upper layers of the Earth's crust. At present, the H_2O-CO_2-NaCl system has thermodynamic models that allow describing its phase state and obtain a number of important thermodynamic characteristics at high temperatures and pressures. This, in particular, is the model by Aranovich et al. (2010). At the same time, such models are not available for the H_2O-CO_2-$CaCl_2$ system.

In this paper we present a thermodynamic model of the H_2O-CO_2-$CaCl_2$ system for high pressures and temperatures, developed on the basis of an equation for the excess free Gibbs energy. The form of the

dependence of the excess Gibbs free energy on the concentration of the components coincides with that proposed for the ternary H_2O-CO_2-NaCl system (Aranovich et al., 2010). In the same paper, the corresponding formulas for calculating the activities of the components of the ternary system are given. In our case, for the temperature T[K], pressure P, and mole fractions of the components $x_1 = x_{H_2O}$, $x_2 = x_{CO_2}$, $x_3 = x_{CaCl_2}$ the excess Gibbs free energy has the form

$$\begin{aligned} G^{mix} &= RT(x_1 \ln x_1 + x_2 \ln x_2 + x_3 \ln x_3) \\ &- x_1 RT \ln[1 + \alpha x_3/(x_1 + x_3)] + x_3\{(1+\alpha)RT \ln(1+\alpha) + \alpha RT \ln[x_3/(x_1 + x_3)] \\ &- (1+\alpha)RT \ln[1 + \alpha x_3/(x_1 + x_3)]\} \\ &+ x_1 x_2 W_1(P,T)\rho(x_1, x_2) \\ &+ x_1 x_3 W_2(P,T) + x_2 x_3[x_2 W_3(P,T) + x_3 W_4(P,T)]/(x_2 + x_3) + x_1 x_2 x_3 W_5(P,T) \end{aligned} \quad (1)$$

The term in the first line of the formula represents the contribution of the entropy of mixing the three components of the system to the Gibbs free energy. The second and third lines represent the contribution of the additional entropy arising due to the dissociation of $CaCl_2$ molecules. α is the degree of dissociation (the average additional number of particles that appeared as a result of the dissociation of one $CaCl_2$ molecule). The value $\alpha_0 = 2$ corresponds to the complete dissociation. The term with the coefficient W_1 describes the interaction of water molecules and CO_2. This term coincides with that of (Aranovich et al., 2010).

$$W_1 = 202046\,\mathrm{J \cdot cm^3/mol},$$
$$\rho(x_1, x_2) = (x_1 + x_2)/(V_1 x_1 + V_2 x_2) \quad (2)$$

V_1 and V_2 are the molar volumes of pure water and carbon dioxide at the given temperature and pressure, respectively.

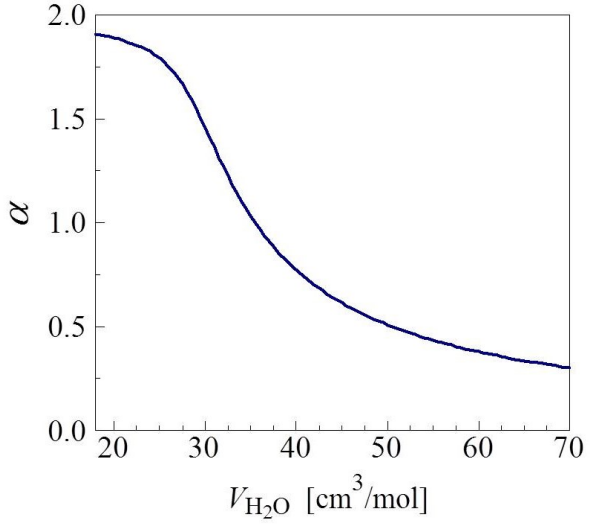

Fig.1. The degree of dissociation of $CaCl_2$ dependent on the molar volume of water at variable temperatures and pressures.

The forms of the dependences on temperature and pressure used by us for the other variables in (1) differ significantly from those used by Aranovich et al. (2010) and are based on a natural parameter for the system under consideration, i.e. the molar volume of water, for which there is an empirical description IAPWS-95 (Wagner, Pruß, 2002), precisely reproducing numerous experimental results.

The degree of dissociation of the $CaCl_2$ molecules should depend on the density of water: when the water density approaches zero, the degree of dissociation should also tend to zero. For a strong electrolyte $CaCl_2$ at a high water density, it is natural to expect the dissociation degree close to the maximum. Since the exact form of the dependence of the degree of dissociation is unknown, we used the formula,

$$\alpha = \frac{\alpha_0}{1 + a^2\left[\sqrt{(V_1 - V_0)^2 + q^2} + V_1 - V_0\right]} \quad (3)$$

This formula corresponds to the qualitative considerations, presented above, and appears to be sufficient for describing the available experimental data. Dependence of the degree of dissociation on the mole volume of water with the values of parameters a, V_0, and q, obtained from the experimental data is shown in Fig. 1. This dependence qualitatively corresponds to the dependence of the degree of dissociation on the mole volume of water, obvious from a priori considerations. On the other hand, this dependence based on a rather limited experimental material and within the framework of a specific thermodynamic model for the ternary H_2O-CO_2-$CaCl_2$ system should not be considered as an independent quantitative description of the degree of dissociation of $CaCl_2$ molecules in an aqueous solution.

The coefficients $W_2,..,W_5$, in the formula for the Gibbs free energy are responsible for the interaction of $CaCl_2$ with H_2O and CO_2. In particular, in the composition diagram, the values of these coefficients determine the position of the boundary, separating the region of the homogeneous fluid from the region of the two coexisting fluid phases. This boundary is represented by a solid line in the Fig. 2, which demonstrates the relationship between the experimental results and the results of our thermodynamic model. Below and to the left of this boundary is the region of a homogeneous fluid, above and to the right is the region of two coexisting phases. The experimental points corresponding to a homogeneous fluid are represented by filled circles, the experimental points corresponding to a two-phase fluid are shown by open circles.

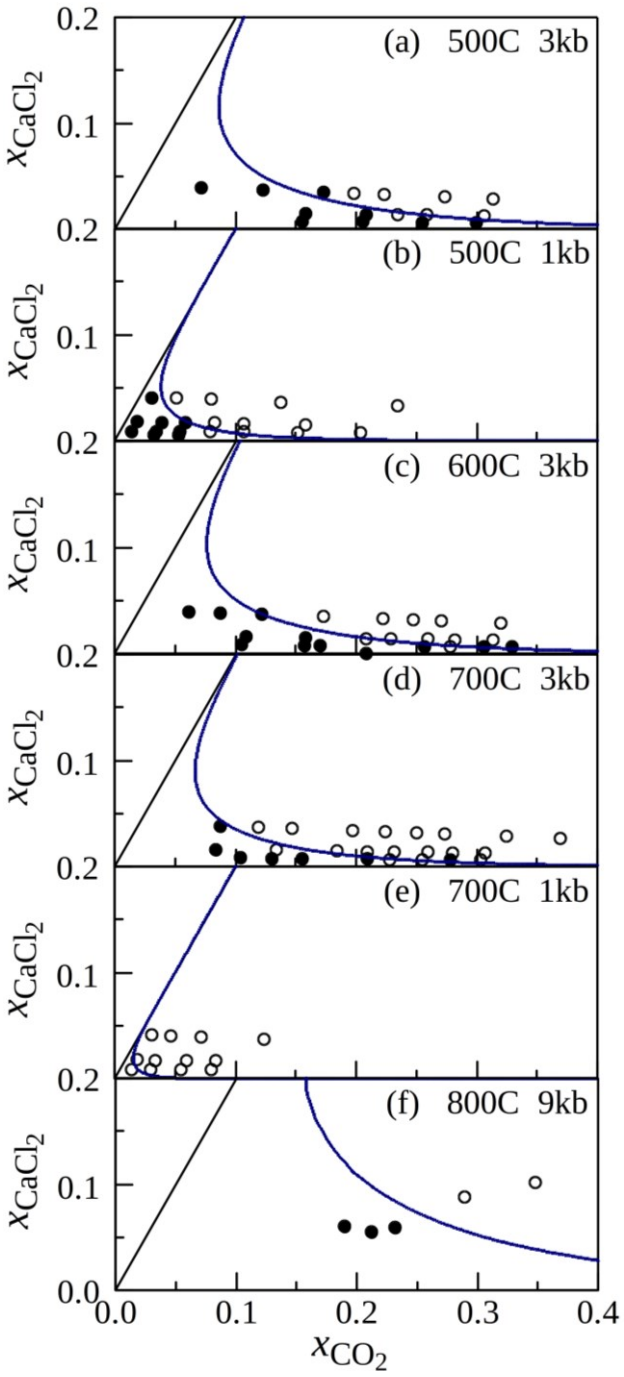

Fig.2. Experimental and our model data on the phase state of the system H_2O-CO_2-$CaCl_2$. Open circles stay for the two-phase fluid, full circles correspond to the homogeneous fluid, curves are boundaries of the region of the homogeneous fluid according our model. Experimental data: (a)-(e) – Zhang, Frantz (1989); (f) – Shmulovich, Graham (2004).

For finding the pressure and temperature dependence of the coefficients $W_2,..,W_5$, corresponding to the experimental data, we carried out a numerical fit of $W_2,..,W_5$, values for each *PT* combination present in the works (Zhang, Frantz, 1989, Shmulovich, Graham, 2004). The Gibbs free energy with these values of $W_2,..,W_5$, gives the boundary between the homogeneous fluid and two-phase fluid, which does not contradict the experimental data. Since the experimental points are sufficiently far from each other and do not form continuous fields, this definition of the values $W_2,..,W_5$, is not unique and serves only as a tool for revealing their *PT* dependencies. Analysis of the data, obtained in this way, showed that it is sufficient to assume a linear dependence of $W_2,..,W_5$, on the mole volume of water to describe the available set of experimental data

$$W_i(P,T) = u_{i0} + u_{i1}V_1(P,T), \quad i = 2,..,5 \qquad (4)$$

Table 1. Numerical values of parameters of our models when using units J, kbar, cm^3, mol, K.

a	8.94694554E-01
V_0	3.88162078E+01
q	3.89103466E+00
u_{20}	2.49162269E+03
u_{21}	3.33471967E+01
u_{30}	-1.86735799E+05
u_{31}	1.54381283E+04
u_{40}	-1.79267486E+05
u_{41}	1.54210444E+04
u_{50}	-8.92808790E+04
u_{51}	4.45755021E+02

The fit of parameters $u_{i0}, u_{i1}, a, V_0, q$ on the experimental data for all available *PT* combinations led to their numerical values given in Tab. 1. For some *PT* points the experimental data and our model boundaries (calculated with parameters of Tab. 1) dividing the region of the homogeneous fluid and the region of two coexisting fluid phases are presented in Fig. 2. In addition to the works (Zhang, Frantz, 1989, Shmulovich, Graham, 2004), experimental data on the system we considered were published by Shmulovich and Plyasunova (1993). Later, these data were critically reviewed by Shmulovich and Graham (2004). According to the explanations given in the last paper, the results by Shmulovich and Plyasunova (1993) contain a significant systematic error, decreasing with increasing temperature. Thus, the results of this work for $T = 773.15$ K are unsuitable for use. Our fit was generally based on experimental data by Zhang and Frantz (1989) and Shmulovich and Graham (2004). However, in view of the extreme shortage in the available experimental data for pressures above 3 kb, we used in our fit also the results by Shmulovich and Plyasunova (1993) for $P = 5$ kb and $T = 973.15$ K, attributing them a much smaller statistical weight.

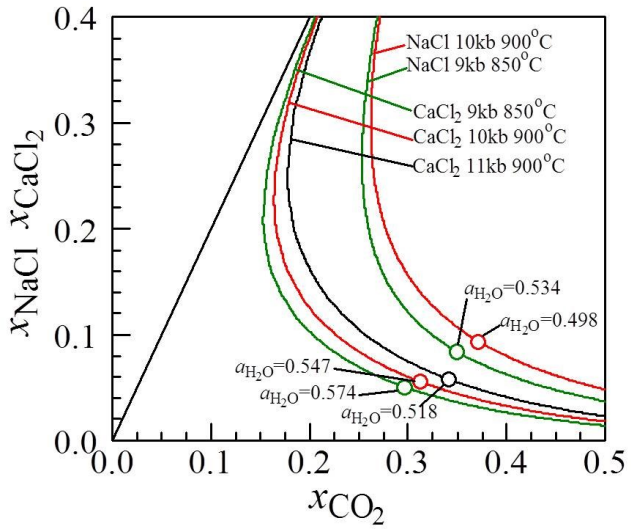

Fig. 3. Boundaries of the heterophase region and the maximum possible values of the water activity in this region for fluids H_2O-CO_2-NaCl and H_2O-CO_2-$CaCl_2$.

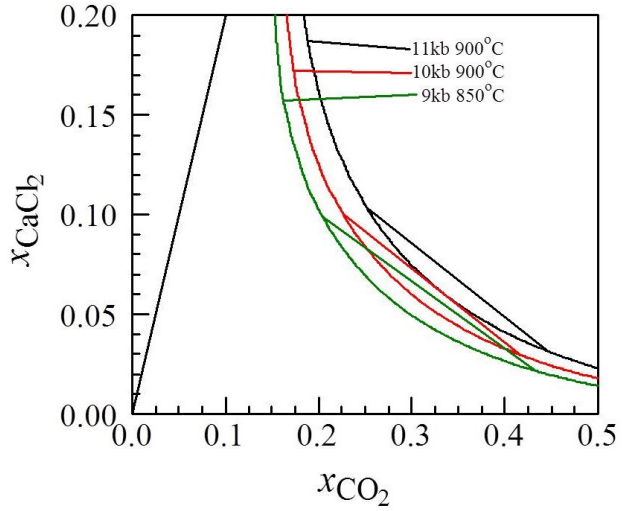

Fig. 4. Conodes, reflecting compositions of coexisting fluid phases of H_2O-CO_2-$CaCl_2$.

The thermodynamic model (1)-(4) with parameters of Tab. 1 reproduces the available experimental data in the temperature range 500-800°C and in the pressure range 1-9 kb. Our parameterization of the *PT* dependences of the coefficients in the Gibbs free energy (1) is based on a natural for this problem and well-known value of the molar volume of water at corresponding *P* and *T*. This makes it possible to apply our model beyond the experimental range of the PT parameters. On the other hand, the question of the completeness of the available experimental data is critically important. It can be seen in Fig. 2 that all available experimental points refer to sufficiently low concentrations of $CaCl_2$, $x_{CaCl_2} < 0.05$ as a rule. This limits the accuracy of our thermodynamic analysis at high concentrations of $CaCl_2$, which are important from the geological point of view. The same insufficiency of the experimental material resulted in the impossibility of application a more advanced form of the Gibbs free energy (Ivanov et al., 2018) to the water-salt part of our system. The appearance of new experimental data should improve the accuracy of the thermodynamic description of fluids with a high $CaCl_2$ concentration.

Our thermodynamic model includes a complete description of the Gibbs free energy. Thus, the knowledge of the numerical parameters of the model makes it possible to calculate the activities of the components of the system. In particular, it is possible to determine the activity of water at the interface boundary between the regions of homogeneous and heterophase fluid, as well as the determination of the compositions of coexisting fluid phases in the heterophase region. The maximal value of the water activity in the heterophase region is an important reference point when analyzing the phase state of the fluid, both on the basis of data on the composition of fluid inclusions and on the results of calculating the activity of water in terms of mineral equilibrium.

The values of these limiting water activities differ significantly for H_2O-CO_2-NaCl and H_2O-CO_2-$CaCl_2$ systems. Comparison of the position of the boundaries of the heterophase region and the maximum possible values of the water activity in this region for H_2O-CO_2-NaCl and H_2O-CO_2-$CaCl_2$ in the *PT* conditions of the granulite facies is shown in Fig. 3. Data for H_2O-CO_2-NaCl were obtained from the model by Aranovich et al. (2010), data for H_2O-CO_2-$CaCl_2$ from our model. At the same temperature and pressure, the two-phase fluid of the H_2O-CO_2-$CaCl_2$ system can coexist with mineral associations corresponding to a higher water activity than that is the case for H_2O-CO_2-NaCl (Bushmin et al., 2017). Fig. 4 shows an example of calculated conodes, reflecting compositions of coexisting fluid phases at *PT* parameters of formation of HP granulites and syngranulitic infiltration metasomatites of the Lapland granulite belt of the Fennoscandian shield (Bushmin et al., 2017).

This research was carried out within the framework of the IPGG RAS research project 0153-2018-0004.

References:

Aranovich L.Ya., Zakirov I.V., Sretenskaya N.G., Gerya T.V. Ternery system H_2O-CO_2-NaCl at high *T-P* parameters: An empirical mixing model. // Geochem. Int. 2010. V.48, P. 446-455.

Bushmin S.A., Vapnik E.A., Ivanov M.V., Lebedeva Y.M., Savva E.V. Fluids of high-pressure granulites: Lapland granulite belt (Fennoscandian shield) // In: Geodynamic conditions and thermodynamic conditions of regional metamorphism in Precambrian and Phanerozoic.

IPGG, Russian Academy of Sciences. St. Petersburg. 2017. P. 40-43.
Ivanov M.V., Bushmin S.A., Aranovich L.Y. // An empiric model of the Gibbs free energy for solutions of NaCl and $CaCl_2$ of arbitrary concentration at temperatures 423.15 K – 623.15 K under vapor saturation pressure. Doklady Earth Sciences 2018. V. 479, Part 2, P. 491–494.
Shmulovich K.I., Graham C.M. An experimental study of phase equilibria in the system H_2O-CO_2-NaCl at 800°C and 9 kbar. // Contrib Mineral Petrol. 1999. V.136. P. 247-257.
Shmulovich K.I., Graham C.M. An experimental study of phase equilibria in the systems H_2O-CO_2-$CaCl_2$ and H_2O–CO_2–NaCl at high pressures and temperatures (500–800°C, 0.5–0.9 GPa): geological and geophysical applications. // Contrib Mineral Petrol. 2004. V.146. P. 450-462.
Shmulovich K.I., Plyasunova N.V. Phase equilibria in ternary systems formed by H_2O and CO_2 with $CaCl_2$ or NaCl at high *T* and *P*. // Geochem. Int. 1993, V. 30, P. 53-71.
Wagner W., Pruß A. The IAPWS formulation 1995 for the thermodynamic properties of ordinary water substance for general and scientific use. // J. Phys. Chem. Ref. Data. 2002. V.31. P.387-535.
Zhang Y.-G., Frantz J.D. Experimental determination of the compositional limits of immiscibility in the system $CaCl_2$-H_2O-CO_2 at high temperatures and pressures using synthetic fluid inclusions // Chem. Geol. 1989. V.74. P. 289–308.

Korepanov[1] Ya.I., Osadchii E.G.[1]. Thermodinamical model of phase diagram Ag-Au-S in atmosperic pressure UDC 550.4.02

[1]*Institute of Experimental Mineralogy RAS, Chernogolovka, Moscow district* yakoff@iem.ac.ru (euo@iem.ac.ru).

Abstract. Based on the literature thermodynamic data for binary and ternary phases and the own data for the Ag_xAu_{1-x} solid solution, the isothermal sections of the Ag-Au-S phase diagram were modeled. Modeling was performed using the program [TernAPI] (laboratory chemical thermodynamics chemical faculty MSU. MSU). For two triple Associations (paragenesises) Ag_2S-Ag_3AuS_2-AgAu and Ag_3AuS_2-AgAuS-AgAu alloys given equilibrium compositions at temperatures 298 K and 423 K. The temperature dependence of the alloy composition in both associations practically the same and is about 2 at% Ag 100 degrees.

***Keywords**: system Ag-Au-S, solid solution, alloy, thermodynamics*

Introduction. Sulphides of gold and silver are present in many gold ore deposits, and the study of their thermodynamic properties is an important study for understanding geochemistry, transport processes and formation of gold deposits.

Using the data available in the literature [Osadchii, Rappo, 2004; Robie, Hemingway, 1995; Korepanov et al., 2013] on the ternary Ag-Au-S system it was possible to calculate the phase diagram using the [TERNAPI] program.

To calculate the phase diagram, temperature dependences of Gibbs energy (Table 1) were used for all existing phases (minerals) in the Ag-Au-S system.

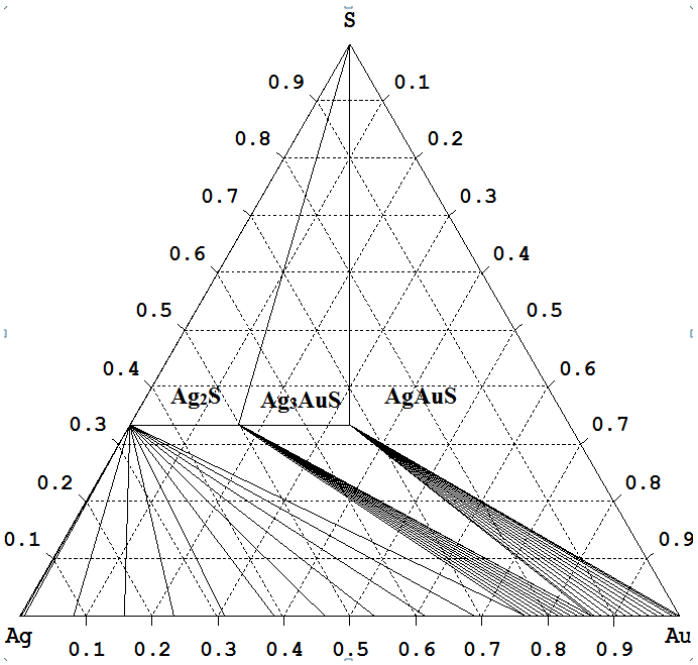

Fig.1. The phase diagram of Ag-Au-S, at a temperature of 423 K

Table 1. Temperature (298.15K-450K) dependences of the Gibbs energy of the phases of the Ag-Au-S system.

Initial data for modeling			
Composition	Mineral	equation	reference
AgAuS	Petrovskite	–24819 –9.3975·*T* (J/mol)	[Osadchii, Rappo., 2004]
Ag_3AuS_2	Uytenbogaardtite	–57287 –40.89·*T* (J/mol)	
Au_2S	Metastable phase	1369 –0.98·*T* (J/mol)	
Ag_2S	Acanthite	-32000 – 25,85·*T* (J/mol)	[Robie, Hemingway., 1995]
Ag_xAu_{1-x}	Native gold	-10^{-3}·96484.56·(590·x^2/3 +350·*x* +200 + 0.1806·*T*)·*x*(1-*x*) (J/mol)	[Korepanov et. al.,., 2013]

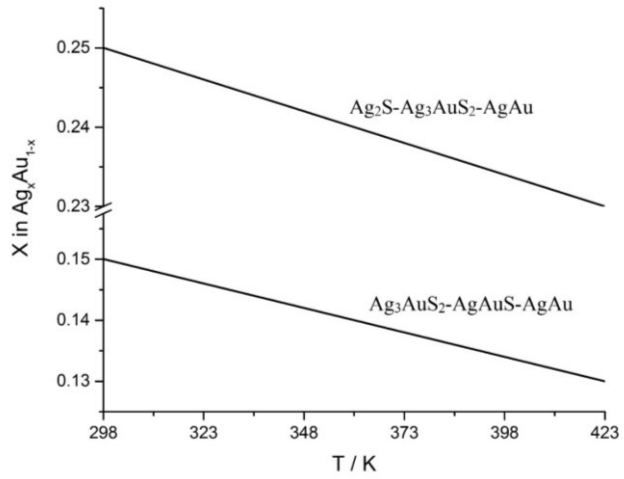

Fig.2. Dependence of the composition of the alloy on temperature in the equilibrium Ag_2S-Ag_3AuS_2-Ag, Au and Ag_3AuS_2-AgAuS-Ag, Au**.**

Table 2. Explored parageneses

Temperature	Triple phase associations	
	Ag_2S-Ag_3AuS_2-Ag,Au	Ag_3AuS_2-AgAuS-Ag,Au
	Alloy composition	
298.15 K	$Ag_{0.25}Au_{0.75}$	$Ag_{0.15}Au_{0.85}$
423.15 K	$Ag_{0.23}Au_{0.77}$	$Ag_{0.13}Au_{0.87}$

The composition of the alloy in the ternary phase associations Ag_2S-Ag_3AuS_2-Ag, Au (Fig. 2) and Ag_3AuS_2-AgAuS-Ag, Au depends on the temperature. This fact can be used to determine the thermodynamic equilibrium of the corresponding parageneses and as a geothermometer, provided that the gold composition is accurately determined at the contact with the double and / or tripartite sulphides.

Supported by program DES RAS Experimental study of mineral equilibria and isotopic ratios

References:

Osadchii E.G., Rappo O.A. (2004) Determination of standard thermodynamic properties of sulfides in the Ag–Au–S system by means of a solid-state galvanic cell. Am Miner 89:1405–1410. doi:10.2138/am-2004-1007

Korepanov Ya.I., Osadchii V.O., Osadchii E.G. New data on the thermodynamics of Ag_xAu_{1-x} solid solution in the temperature range 323-673K // Experimental geochemistry. - 2013. - T. 1, No. 5. - C. 1-4.(in Russian)

Robie, R.A. and Hemingway, B.S. (1995) Thermodynamic properties of mineralsand related substances at 298.15 K and 1 Bar (105 Pascals) pressure and at high temperatures. U.S. Geological Survey Bulletin 2131.

The TernAPI program is designed to calculate the phase diagrams of ternary systems by the convex hull method. http://td.chem.msu.ru/develop/ternapi/

Korepanov Ya.I.[1], Osadchii E.G.[1] Determination of thermodinamical properties of alloy Ag_xAu_{1-x} in temperature range of 323 – 673 K and atmospheric pressure by EMF method using Ag β`-alumina as a solid state electrolite UDC 550.4.02

[1] Institute of Experimental Mineralogy RAS, Chernogolovka, Moscow district yakoff@iem.ac.ru euo@iem.ac.ru

Abstract During the study, the temperature dependence activity of silver in alloy (Ag_xAu_{1-x}) for 6 compounds was determined by the EMF method in the range of 323 - 623 K and atmospheric pressure of argon with high reproducibility of the results (3% of the absolute value). As a solid electrolyte, Ag + conducting ceramics (Ag β'-alumina, Ionotec LTD England) was used. Experimentally, high stability and repeatability of data in electrochemical cells using silver-conducting ceramics were shown.

To describe the results array of data, an equation of the form:

$$ln(a_x) = -n \cdot F \cdot (A \cdot x^2 + B \cdot x + C(T))(1-x)^2/(R \cdot T) \quad (1)$$

Approximation of the data by equation (1) with accurately describes the experimental data and allows us to calculate the activity of the second component (Au) using the Gibbs-Diugem equation.

Keywords: *Ag-Au, alloy, thermodynamics, metals and alloys, solid solution, EMF, gold, silver, thermodynamics, activity.*

Introduction At the moment there are an impressive amount of works related to the study of the properties of the AgAu alloy [Okamoto, Massalski 1983; Barker et al., 1983; Fischbach 1980; Osadchii et al., 2016; White et al. 1957; Stanley, Huggins, 1971] with the references. One of the most important aspects of the study is determination of the thermodynamic parameters of alloy. As a rule, this is a direct determination of activity of silver by the EMF method with further description and calculation of the thermodynamic parameters [Okamoto, Massalski, 1983; Barker et al., 1983; Fischbach, 1980; Osadchii et al., 2016]. Last works in this field were made in the early 1980s using silver-conducting ceramics as an electrolyte [Barker et al., 1983; Fischbach, 1980], but the data presented in them are presented in such a way that further use in detailed calculations is not rational. The most interesting and reliable work on the thermodynamics of gold - silver alloy, both from the point of view of the data and in terms of generalizations and descriptions available at the time in the literature, is the article White with co-authors published in 1957 [White et al., 1957].

Available data on the thermodynamics of AgAu alloy have not particular value for simulation of ternary phase diagrams, such as Ag-Au-Chalcogen, since the choice of one or another source gives a significant difference in the construction of the phase

diagram. On the basis of these facts, it was decided to study the thermodynamics of the Ag-Au alloy in detail and obtain an experimental technique that makes it possible to obtain repeatable results regardless of the external conditions.

The main problem of electrochemistry is the exclusion of processes not related to the research. In the case of EMF measurements in a solid-state galvanic cell, this problem is reduced to the choice of an inert atmosphere (argon current) and electrolyte with high conductivity of the ions participating in the reaction and minimal electronic conductivity. To substantiate the applicability of the solid electrolytes used, a number of experiments and literature analysis have been carried out which showed that the iodine-containing electrolytes (AgI, $RbAg_4I_5$) used for EMF measurements react with the alloy, which leads to the impossibility of interpreting the results obtained. Thus, to study the properties of the alloy, only AgCl and Ag β'-alumina are applicable. A detailed comparison of the characteristics of silver-conducting solid electrolytes and evidence of applicability, as well as a description of the advantages of Ag β'-alumina, is given in the article [Stanley, Huggins 1971].

Experiment and Results. Samples

Gold and silver foil (99.95%) were used to make the samples. The samples were manufactured in two stages: first, the alloy of the given weight and composition was homogenized in the evacuated ampoule in the flame of the gas burner, then the necessary shape was given in the mold, followed by annealing the tablets in an evacuated ampoule at a temperature of 873 K for 10 days, followed by a smooth controlled by cooling for 10 days.

Ceramics of Ag β'-alumina provided by Ionotec LTD England in the form of a disc of 45 mm in diameter and 1.5 mm thick was given the shape of a cylinder 6 mm in diameter using inert abrasive tools.

Solid state galvanic cell for EMF measurements

An electrochemical cell for determination EMF is a column consisting of a reference electrode (Ag), an investigated alloy (AgAu) and an electrolyte between them, with current leads and the corresponding construction. The design of the installation and the procedure for conducting the experiment are described in detail in the article [Osadchii, Rappo 2004].

Elements of the cell (Fig.1.) Are placed in the form of a column cell holder (6.5 mm inside diameter) and are pressed by a spring for the reliability of electrical contacts. The cell holder is placed in a quartz glass container with gas inlet and outlet connections. The measurements are carried out in a dry argon flow (flow rate 0.5-1 cm^3 / min).

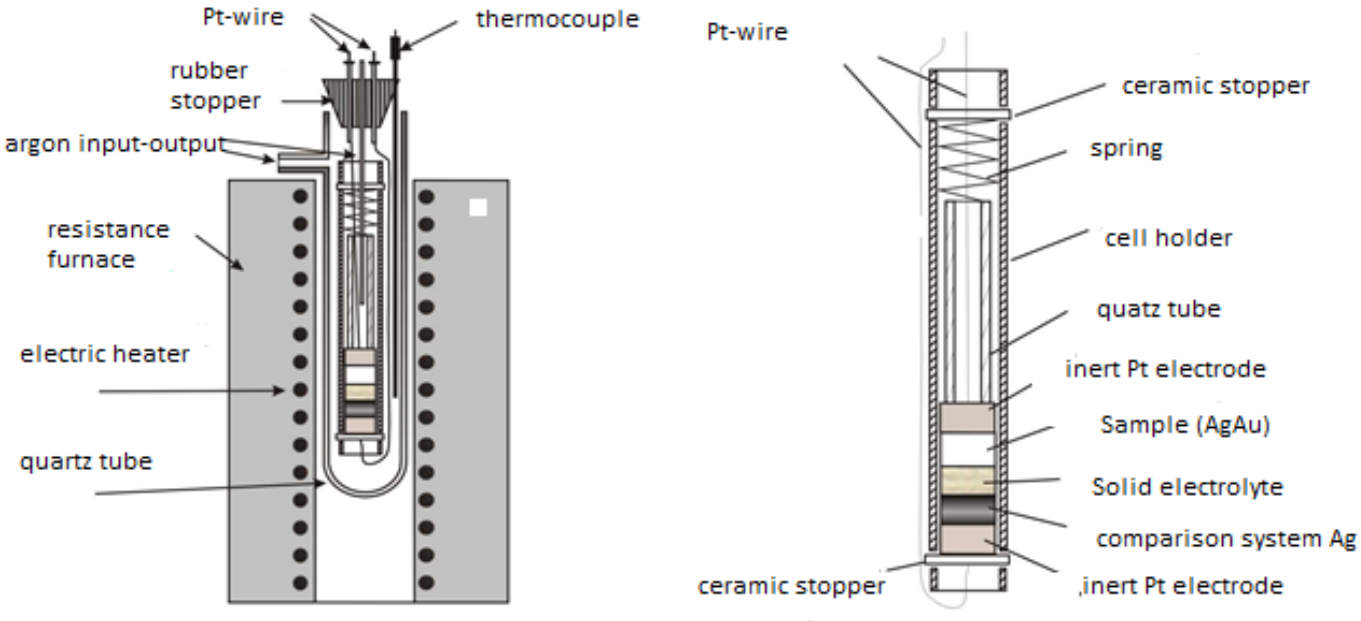

Fig.1. Scheme of electrochemical cell

Achieving the equilibrium EMF value took from 1 hour to 10 days for different temperatures and compositions. The equilibrium was considered achieved when the EMF values remained unchanged within ± 2.5% of the absolute value of the EMF value during the day.

The temperature dependences of the EMF are determined in a reversible galvanic circuit

$$(-)\ \mathrm{Pt|C(graphite)|Ag|AgCl\ or}$$

$$\mathrm{Ag-\beta' alumina\ |Ag_xAu_{1-x}|C(graphite)|Pt}\ (+)$$

with Ag β'-alumina or AgCl as a solid electrolyte.

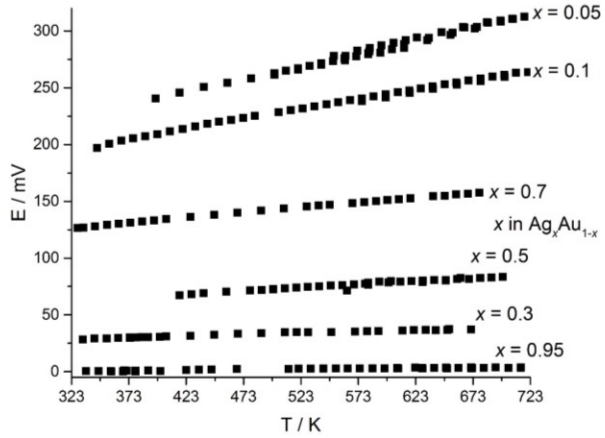

Fig.2. EMF dependence for the test compositions as a function of temperature.

Supported by program DES RAS Experimental study of mineral equilibria and isotopic ratios.

References:

Okamoto H. and T. B. Massalski, The Ag-Au (Silver-Gold) System, Bull. Alloy Phase Diagrams, 1983, 4, 30–38.

Barker WW, R Browner, FJ Lincoln The System Silver--Gold: The Reproducibility of Silver Activity Measurements Using the Solid Ionic Conductor, Silver--Beta-Alumina - Proc. Australas. Inst. Min. Metall., 1983

Fischbach H., "EMF-Measurements on Ag−Au-Alloys Employing Ag-β-Alumina", Z. Metallkd., 71(7), 448–450 (1980) in German. (Thermo; Experimental)

Osadchii E.G., Korepanov Y.I., Zhdanov N.N., A multichannel electrochemical cell with glycerin-based liquid electrolyte, Instruments and Experimental Techniques. 2016. T. 59. № 2. C. 302-304

Osadchii E.G., Rappo O.A. (2004) Determination of standard thermodynamic properties of sulfides in the Ag–Au–S system by means of a solid-state galvanic cell. Am Miner 89:1405–1410. doi:10.2138/am-2004-1007

White J. L., Orr R. L., Hultgren R (1957) The thermodynamic properties of silver-gold alloys, Acta Mater 5: 747-760.

Stanley M. Whittingham, Robert A. Huggins., Transport Properties of Silver Beta Alumina, J. Electrochem. Soc.: ELECTROCHEMICAL SCIENCE January 1971. doi:10.1149/1.2407944

Kovalskaya T.N., Varlamov D. A., Shapovalov Y.B., Kalinin G.M., Kotelnikov A.R. Experimental study of postmagmatic processes in Tiksheozerskiy massif UDC 552.11; 552.3

Korzhinsky Institute of Experimental Mineralogy RAS, Chernogolovka, tatiana76@iem.ac.ru *tatiana76@iem.ac.ru* , *dima@iem.ac.ru*, *shap@iem.ac.ru*, *garik@iem.ac.ru*, *kotelnik@iem.ac.ru*

Abstract. The Tiksheozero massif belongs to the formation of ultrabasic alkaline massifs with carbonatites, but it is located to the south of the main cluster of carbonatite massifs of the Karelian-Kola province, in the circumpolar part of North Karelia, to the south of the city of Kandalaksha. The literature data indicate estimates of the age of the massif in the interval 1.8-1.9 billion years, which sharply differs from the other alkaline-carbonatite complexes of the Karelian-Kola province, whose age is estimated as the Middle Paleozoic. A detailed study of the rocks of the massif showed that most rocks are subject to postmagmatic changes with increasing potassium content in the rock - potassium minerals - richterite, feldspar, etc. appear. Previous experimental studies have shown that the Tiksheozero massif underwent significant postmagmatic changes. In order to simulate the conditions of postmagmatic changes, experiments were conducted on the interaction of the rock (ground gabbro) with the fluid. As the fluid, 1M KF solution was taken in the ratio by weight to the sample in the ratio 1:10. The synthesis was carried out in two stages: in platinum ampoules heating to 1100 ° C and pressure 3 kbar and holding at these parameters for 5 hours. Then isobaric cooling to 850°C. The duration of the experiment was 10 days. As a result of the experiments, amphiboles were obtained, convergence and composition with amphiboles from the nominal gabbro massif.

Keywords: *carbonatite massifs, amphibolization, postmagmatic changes, fluid, clinopyroxenes.*

The Tiksheozero massif belongs to the formation of ultrabasic alkaline massifs with carbonatites, but it is located to the south of the main cluster of carbonatite massifs of the Karelian-Kola province, in the circumpolar part of North Karelia, to the south of the city of Kandalaksha (Kukharenko et al., 1969). Unlike the well-known alkaline massifs with carbonatites of the Caledonian-Hercynian period (the Kovdor massif and others), the Tikshoozero massif belongs to the earliest Proterozoic subplatform complex on the territory of the Fennoscandian Shield. The literature data indicate estimates of the age of the massif in the interval 1.8-1.9 billion years, which sharply differs from the other alkaline-carbonatite complexes of the Karelian-Kola province, whose age is estimated as the Middle Paleozoic (Metallogeny ..., 2001).

The carried out analysis of the literary material showed that, in the petrological sense, the array has been poorly studied; its study was mainly connected with the search for mineral deposits and was carried out in 1980-1990. The Tikshozero massif is a round-elliptical body with a diameter of the order of 20 km, and is composed of olivinites, gabbro, pyroxenites (sometimes with nepheline), ijolites, carbonatites, amphibole-calcite-cancrinite rocks. Carbonatites of the mass form stock-like bodies tens of meters in size, eruptive breccia-shaped structures, veins and veins. The largest body of carbonatites of the Tiksheozersky massif was traced to the depth of 450 m. Apatite calcite ores of the complex type were found in the carbonatites of the massif (Metallogeniya ..., 2001).

In order to determine the features of mineralogens of alkaline rocks of the Tiksheozero massif and their difference from the rocks of other alkaline-carbonatite complexes of the Karelian-Kola province, we conducted a study of the chemical compositions of rock-forming and accessory minerals in the rocks samples of the Tiksheozero massif and carried out a paragenetic analysis. In the course of the work, samples of the core material stored in the village were analyzed. Chupa and in the Geological Institute of KarRC RAS (Petrozavodsk), as well as samples of rocks selected during expedition work of three field seasons directly on the massif. The samples of olivinites, carbonatites, pyroxenites, gabbros, syenites (including nepheline) and yiolite-urtites of the Tiksheozero massif are studied.

The rocks of the Tiksheozero Massif Olivinites within the Tikshozero massif occupy no more than 10% of the total volume of rocks, however, they are usually considered to be the earliest phase of the introduction during the formation of the massif (Kukharenko et al. 1969). The olivinite body is located in the central part of the massif. These are rocks with medium-grained cumulative structure and massive texture, composed of olivine, clinopyroxene, amphibole, serpentine, chlorite, chromite, titanomagnetite, copper, iron, nickel and cobalt sulfides as accessory minerals. With microscopic observation, it was established that the grains of olivine are subidiomorphic in shape, their size reaches 3 mm; grains of clinopyroxene are also subidiomorphic, their size reaches 1.5 mm. In the interstices between the clinopyroxene and olivine grains, there are grains of sulphides, titanomagnetite, chromite and amphibole. Most of them have a xenomorphic appearance, the size does not exceed 0.3 mm, although in some cases "phenocrysts" of subordiomorphic chromite grains have been encountered in serpentine mass. In the interstices, serpentine is also found, in some cases it replaces up to 90% of the primary olivine.

Pyroxenites are rocks of massive texture and small- and medium-grained structures. They are composed mainly clinopyroxenes (diopside-hedenbergite and aegirine-augite), phlogopite, amphiboles, sphene, carbonate (calcite). As accessory minerals, apatite and ilmenite are present, in some samples orthite is observed. Clinopyroxene is observed in the form of subidiomorphic tabular grains, up to 1-1.5 mm in size, often these grains are resorbed or partially replaced by aggregates of secondary minerals. The phlogopite in the samples studied is represented by subidiomorphic grains; their size is about 0.5 mm. The interstitium between the clinopyroxene and phlogopite grains is filled with intergrowths of ilmenite and calcite. The ilmenite grains are xenomorphic, their size ranges from 0.05 to 0.5 mm. Calcite in interstitiums is aggregates of xenomorphic grains, up to several tenths of a mm in size. Sometimes in the intervals between calcite and ilmenite there are small (up to 0.1 mm) grains of orthite, amphibole, apatite. Most of the samples of pyroxenites studied have been greatly altered - carbonates (calcite with a mole fraction of strontianite up to 1% and dolomite to 1%) are present in the rocks in large quantities, as well as low-temperature minerals such as natrolite, sodalite and cancrinite. Gabbro have a massive texture and a fine-grained structure. The gabbro structure as a whole is similar to the structure of clinopyroxenite. They are folded by clinopyroxene (aegirine-augite), plagioclase (An55), amphibole, phlogopite is present in some samples.

As an accessory mineral, ilmenite and apatite are present. In gabbro, as well as in pyroxenites, there are strong secondary changes - carbonatization, the appearance of low-temperature minerals - zeolites. The amphibolization of clinopyroxenes is the most active in the gabbro - all grains have rims of the alkaline amphibole, corresponding to the composition of pargasite; sometimes amphiboles almost completely replace the seeds of clinopyroxene (Figure 1).

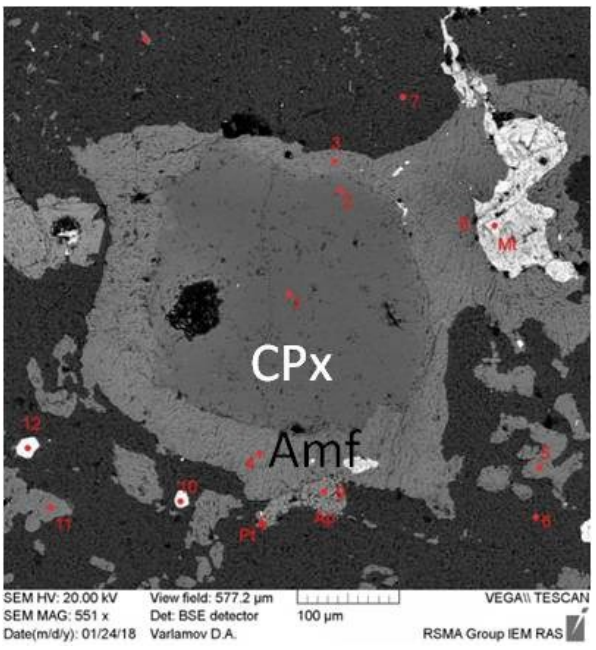

Fig. 1. Clinopyroxene with an amphibole rim. Gabbro. Tiksheozero massif.

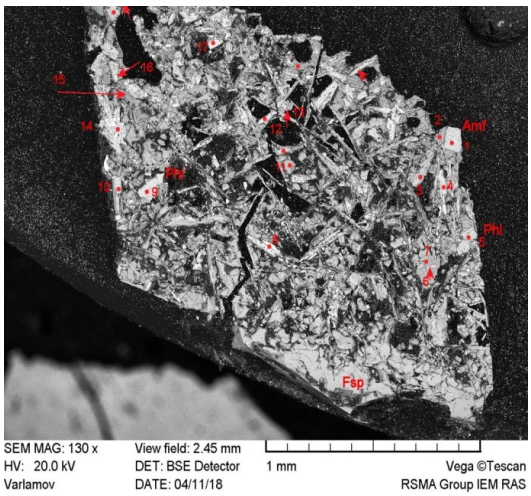

Fig. 2 Products of gabbro amphibolization experiments.

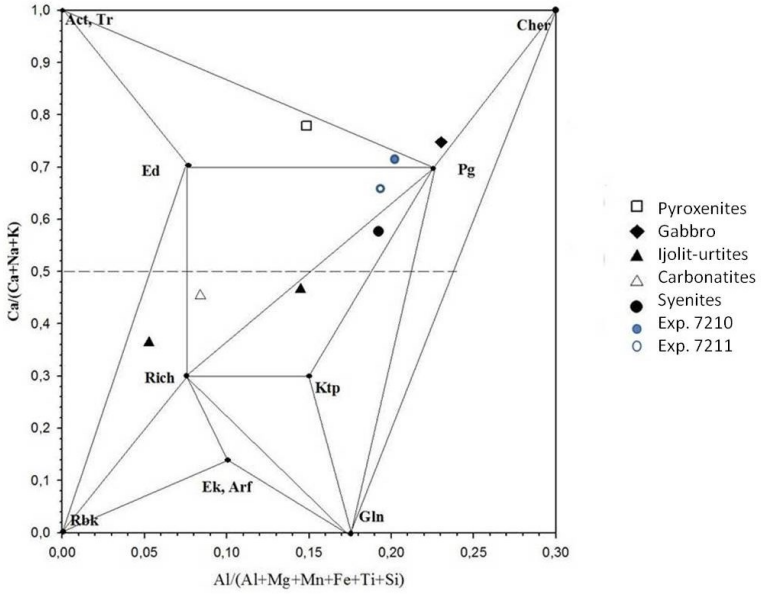

Fig. 3. Amphiboles of Tiksheozersky massif

Alkaline rocks in the Tikshozero massif are represented by iiolite-urtites, syenites, and nepheline syenites. Iiolite-urtites are medium-grained rocks composed mainly of clinopyroxene, phlogopite, nepheline, and potassium feldspar. Muscovite is found in some samples. The size of individual grains is up to 3-5 cm. When microscopic examination of the samples, it is established that nepheline accumulations are observed between the grains of clinopyroxene and phlogopite. As accessory minerals in iiolite-urtites, apatite, sphene, ilmenite are present. The amphiboles of the Tiksheozero massif are extremely diverse in composition, but they all refer to alkaline amphiboles. They are observed in olivinites, pyroxenites, gabbro, and yolite-urtites, and as secondary minerals in carbonatites. The amphibole compositions of the Tiksheozero massif are shown in Table 2. As shown in Fig. 3, amphiboles of different compositions occur within the same rock, which is a consequence of a change in the physicochemical conditions of rock formation and the potential of alkaline components. In earlier parageneses, more calcium amphiboles were encountered, and in the subsequent parageneses alkaline amphiboles appeared, which in composition corresponded to the Richterite and the cataphorite (Figure 3), which is a consequence of the accumulation of alkalis in the melt and a decrease in the crystallization temperature of the melt (Seredkin et al., 2002). With an increase in the aegirine component in clinopyroxenes, the calcium content decreases (the proportion of sodium increases) in amphiboles. This also indicates an increase in alkalinity during the general evolution in the formation of the massif (Perchuk, Ryabchikov, 1976).

Table 1. The gabbro composition of Lucculaisvaara massif.

SiO_2	49.27
TiO_2	1.03
Al_2O_3	13.43
Cr_2O_3	0,13
FeO*.	14.94
Lucculaisvaara MnO	0.14
MgO	5.21
CaO	6.24
Na_2O	4.35
K_2O	1.81
Total	99.56

Experiment on modeling of gabbro amphibolization. In order to recreate the conditions for the formation of postmagmatic changes in the gabbro, experiments were carried out to simulate gabbro amphibolization, since amphibole fringes around clinopyroxenes were found in gabbro samples from the Tiksheozero massif (Fig. 1). As the initial components in the experiments, we took: a ground gabbro from the array of Lucculaisvaara (Table 1), KF 1M and 2 M solutions in a ratio of 1:10 to the weight of the sample. The duration of the experiments was 10 days. First, the reaction mixture was heated to 1100^{o}C and P = 3 kbar, kept at these parameters for 1 hour, then wasobaric cooling to 850 ^{o}C, P = 3kbar followed by holding for 10 days at these parameters. For the experiment we used platinum ampoules with a diameter of 5 mm. The experiments were carried out on a high pressure gas installation. The products of the experiments were a fine-grained mass of greenish-gray color (Figure 2). A study using a microprobe CamScan MV2300 showed that amphiboles formed in the experiments from the grinded gabbro massif of Luqqulaisvaara were similar in composition to the amphiboles of the Tiksheozero massif of the pargasite group (Fig. 3, Table 2).

Table 2. The average chemical composition of amphiboles from the rocks of the Tiksheozero Massif.

	T176-140	T7	t158-203	t158-210	t158-213	t158-203	Amphibole (synth.)
SiO_2	44.08	41.33	43.27	49.10	40.21	51.91	43.18
TiO_2	0.48	0.06	1.41	0.91	1.07	0.94	1.32
Al_2O_3	11.20	17.28	10.91	6.53	14.30	4.06	12.78
FeO	16.43	20.44	18.57	13.23	19.38	13.75	12.94
MnO	-	0.13	-	-	0.19	0.09	0.25
MgO	11.81	6.36	10.81	15.60	9.06	14.70	12.32
CaO	13.47	11.96	9.05	8.68	10.93	7.30	12.14
Na_2O	1.29	1.85	5.16	5.43	3.57	6.66	2.24
K_2O	1.24	0.58	0.81	0.52	1.30	0.59	1.83
Σ	100.00	100.00	100.00	100.00	100.00	100.00	100.00

Note: - under determination limit, synth – synthtetic.

On the basis of the obtained data, it is possible to assume two variants of coexistence of pyroxenes and amphiboles in rocks of the Tiksheozero massif:

1. Natural amphiboles encountered in rocks along with pyroxenes are not paragenetic with them.
2. Natural amphiboles encountered in rocks together with pyroxenes have been altered (with increasing Ca content) during the evolution of the massif, possibly during carbonatization and development of the K-containing fluid.

In favor of the second assumption is the presence in all these rocks along with pyroxene and amphibole and essentially calcium carbonate, as well as the presence of potassium minerals and the results of experimental studies.

References:

Kukharenko A.A., Orlova M.P., Bagdasarov E.A. Alkaline gabbroids of Karelia. Leningrad: Leningrad State University, 1969, 184 p. (in Russian).

Metallogeny of magmatic complexes of intraplate geodynamic environments. Moscow: GEOS, 2001, 640 p. (in Russian)

Perchuk L.L, Ryabchikov I.D. Phase matching in mineral systems. M .: Nedra, 1976, 287p. (in Russian)

Seredkin M.V., Zotov I.A., Karchevsky P.I. Mineralogical types of calcite carbonatites of the Kovdor massif on the Kola Peninsula and their genetic interpretation // Dokl. RAS. 2002. T. 383. № 4. P.532-536. (in Russian).

Shornikov S. I. Investigation of thermodynamic properties of spinel solid solutions by Knudsen effusion mass-spectrometric method

V. I. Vernadsky Institute of Geochemistry and Analytical Chemistry RAS, Moscow (sergey.shornikov@gmail.com)

Abstract. The partial pressure values of the gas phase components over the spinel solid solutions and its border were determined by the Knudsen effusion mass-spectrometric method in the temperature range 2000–2200 K. The found values of the oxide activities, the Gibbs energy, enthalpy and entropy of formation of solid solutions indicated the minor negative deviations from ideality. The obtained thermodynamic information associated with available in the literature.

Keywords: *spinel solid solutions, evaporation, thermodynamic, Knudsen effusion mass spectrometry.*

The study of spinel and its solid solutions, which are part of multicomponent systems, is interesting for petrology, as well as for cosmochemistry, as a mineral of refractory Ca–Al Inclusions (CAIs) often found in carbonaceous chondrites. CAIs are the earliest object of the Solar system with unusual isotopic characteristics (Wark & Boynton, 2001). The Fig. 1 shows the adopted $MgO–Al_2O_3$ system phase diagram according to the data (Berezhnoi, 1970; Ronchi & Sheindlin, 2001), where you can see a wide area of solid solutions.

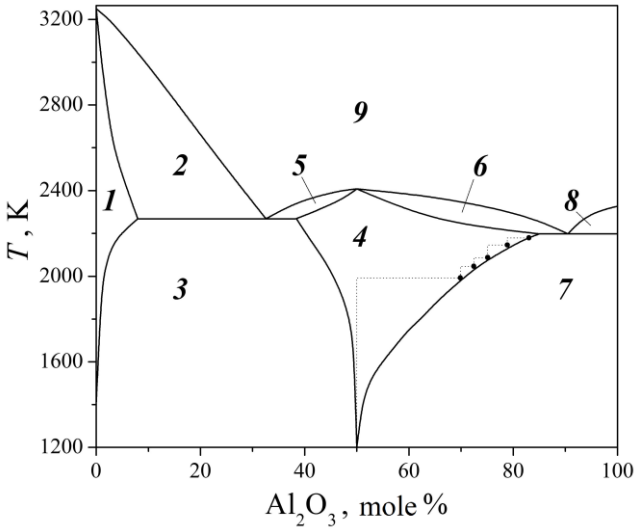

Fig. 1. The phase diagram of the $MgO–Al_2O_3$ system: *1* – MgO (solid solution); *2* – MgO + liquid; *3* – MgO (solid solution) + $MgAl_2O_4$; *4* – $MgAl_2O_4$ (solid solution); *5* и *6* – $MgAl_2O_4$ + liquid; *7* – $MgAl_2O_4$ + Al_2O_3; *8* – Al_2O_3 + liquid; *9* – liquid. The symbol positions on the boundary of phases of *4* and *7* were defined by the Knudsen effusion mass-spectrometric method at present study.

Evaporation processes and thermodynamic properties of MgO and Al_2O_3 have been studied in detail (Glushko et al., 1978–1982). The gas phase over magnesium oxide consists of molecular components – O, O_2, O_3, O_4, Mg, MgO and Mg_2, and over aluminum oxide – O, O_2, O_3, O_4, Al, AlO, AlO_2,

Al_2, Al_2O, Al_2O_2 and Al_2O_3. Earlier, the evaporation of $MgAl_2O_4$ spinel was studied by Knudsen mass spectrometry effusion method at 1850–2250 K. In addition to the listed components of the gas phase, a complex MgAlO gaseous oxide was found in a small amount (Shornikov, 2017a). The values of the oxide activities and the Gibbs energy of $MgAl_2O_4$ stoichiometric spinel were determined at 1851–2298 K. The enthalpy and entropy of spinel formation (from simple oxides) were equal to –12.02±1.14 kJ/mole and 5.03±0.56 J/(mole·K), respectively. The melting enthalpy of spinel was equal to 55.81±4.62 kJ/mole (Shornikov, 2017b), that is satisfactorily consistent with literature thermodynamic information. The information on solid spinel solutions (in contrast to the same on oxides and stoichiometric spinels) is rather scarce and is exhausted by modest results of several experimental investigations.

At present study the thermodynamic data on the properties of spinel solid solutions in the $MgAl_2O_4$–Al_2O_3 system were obtained by the Knudsen effusion mass–spectrometric method at stationary evaporation of stoichiometric spinel sample from a molybdenum cell in the temperature range 2000–2200 K. The MI–1201 mass spectrometer was equipped with a modified high-temperature ion source (up to 3000 K). The design of the developed ion source and the mass spectrometry experiment features are described in detail (Shornikov et al., 2000). The stoichiometric spinel synthesis was carried out by sintering of active ultrafine powders obtained by the joint crystallization method of nitrates and sulphates of magnesium and aluminum, as well as by solid-phase synthesis. The mixtures compositions were prepared with stoichiometric ratio of magnesium and aluminum oxides followed by x-ray phase and chemical analyses of spinel samples.

We can omit the MgAlO low contents in the gas phase, and than the stoichiometric spinel evaporation process can be conditionally presented as the following reaction:

$$2[MgAl_2O_4] = (Mg) + (MgO) + (Al) + (AlO) + (Al_2O) + 3(O) + (O_2). \quad (1)$$

This gives us the opportunity to obtain the compositions of spinel solid solution directly in effusion cell at evaporation due to the Mg preferential evaporation. In this case, the composition change of the spinel residual melt can be calculated by the complete isothermal evaporation method (Sidorov et al., 1985). According to these method, the measured intensities of the ion currents (I_i) belonging to the ith oxides depend on the evaporation time (t), and determine the amount of the evaporated oxide (q_t) contained in the spinel solid solution:

$$q_t = q_0 \frac{\int_{t=0}^{t} I_i dt}{\int_{t=0}^{t=t_0} I_i dt}, \quad (2)$$

where I_i is the total ion current of the ith melt component (MgO or Al_2O_3); t_0 is the complete evaporation time of the i-th component quantity of q_0. Note that the change in the spinel composition during evaporation continued until the compositions located at the boundary of the spinel solid solutions and the "$MgAl_2O_4$ + Al_2O_3" region. When the boundary composition of the solid spinel solution (x_i^*) is reached, its congruent evaporation was observed. It allowed to determine the boundary position, choosing the temperature experiment conditions. In particular, the boundary position was 70.40±0.20 mole % Al_2O_3 at 2000 K, 76.25±0.20 mole % Al_2O_3 at 2100 K, and 84.40±0.20 mole % Al_2O_3 at 2200 K.

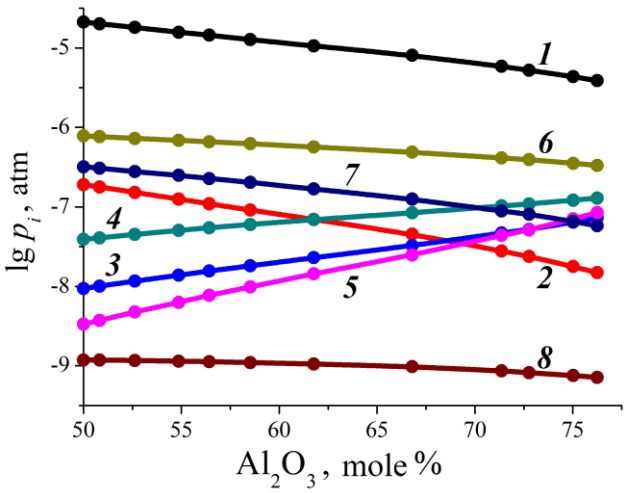

Fig. 2. The partial pressure values of vapor species over spinel solid solutions at 2100 K. Table of symbols: *1* – Mg; *2* – MgO; *3* – Al; *4* – AlO; *5* – Al_2O; *6* – O; *7* – O_2; *8* – MgAlO.

The partial pressure values of vapor species over spinel solid solution (p_i) given in Fig. 2 were determined by the Hertz-Knudsen equation:

$$p_i = K_\alpha \frac{q_i}{s_{or} C_{or} t} \sqrt{\frac{2\pi RT}{M_i}}, \quad (3)$$

where q_i is the component quantity with molecular weight (M_i) evaporated from the effusion cell at temperature of T through the effusion orifice, characterized by the Clausing's factor of C_{or} and the orifice area of s_{or} (Shornikov, 2002). K_α constant value takes into account the α_i evaporation coefficient of ith component. α_i associated with

structure changes of molecule during its transition into the gas phase from the surface with an area of S_v. K_α was calculated using the Komlev's equation (Komlev, 1964):

$$K_\alpha = \frac{1}{C_{or}} + s_{or}\frac{1-C_c\alpha_i}{S_v\alpha_i C_c}, \quad (4)$$

where C_c is the Clausing's coefficient for effusion cell. C_c is associated with the vapor species collisions inside the channel of the effusion orifice of cell and their reverse reflection from the channel walls. Their value does not exceed 1 and depends on the ratio of the effusion orifice diameter to its thickness. Taking into account the prevalence of vapor species typical for MgO and Al_2O_3 and a small amount of MgAlO over spinel, the values of partial evaporation coefficients were taken in (Shornikov, 2015).

Oxide activities in spinel solid solutions (Fig. 3) were determined from the p_i values according to Lewis's equation (Lewis & Randall, 1923) and to the Gibbs-Duhem equation (Prigogine & Defay, 1954), as well as considering the proportionality of p_i values corresponding I_i values, using the Belton-Fruehan method (Belton & Fruehan, 1971):

$$\ln a_{MgO} = \ln a^*_{MgO} - \int_{x^*_{Al_2O_3}}^{x_{Al_2O_3}} \frac{x_{Al_2O_3}}{1+x_{Al_2O_3}} d\ln\frac{I_{Al}I_{AlO}}{I^2_{Mg}} \quad (5)$$

$$\ln a_{Al_2O_3} = -\int_{x^*_{MgO}}^{x_{MgO}} \frac{x_{MgO}}{1-x_{MgO}} d\ln\frac{I_{Mg}I_{Al_2O}}{I^2_{Al}}, \quad (6)$$

where a^*_{MgO} is activity of MgO in stoichiometric spinel at a given temperature ($x^*_{Al_2O_3}$ = 0.5); x^*_{MgO} is the MgO content in the boundary composition of the spinel solid solutions and the "$MgAl_2O_4$ (solid solution) + Al_2O_3" field.

The MgO activities found at present study (Fig. 3*a*) are average between the results (Sasamoto et al., 1981; Fujii et al., 2000). Some excess of the MgO activities (Sakamoto et al. 1981) are due to ignoring of the difference between the partial pressure of oxygen over MgO and the same over the spinel solid solutions in the calculation. The relatively low values of MgO activities (Fujii et al., 2000) are apparently due to errors in determining the boundary composition positions, which were used in the calculations of the oxide activities in spinel solid solutions. The calculated Al_2O_3 activities at 1400–2173 K (Navrotsky et al., 1986) are quite far from the results (Fujii et al. 2000) and the results of present study (Fig. 3*b*). It is probably due to significant calculation errors.

A summary of partial ($\Delta\mu_i$, ΔH_i, ΔS_i) and integral (ΔG_T, ΔH_T, ΔS_T) thermodynamic functions of spinel solid solutions calculated at present study at 2100 K is given in Fig. 4. It can be seen their simbanet behavior in dependence on the oxide contents, that is indicate the slight negative deviations from ideality. It is seen that the integral thermodynamic characteristics are almost unchanged in the spinel solid solutions and their extreme values are in the stoichiometric spinel composition.

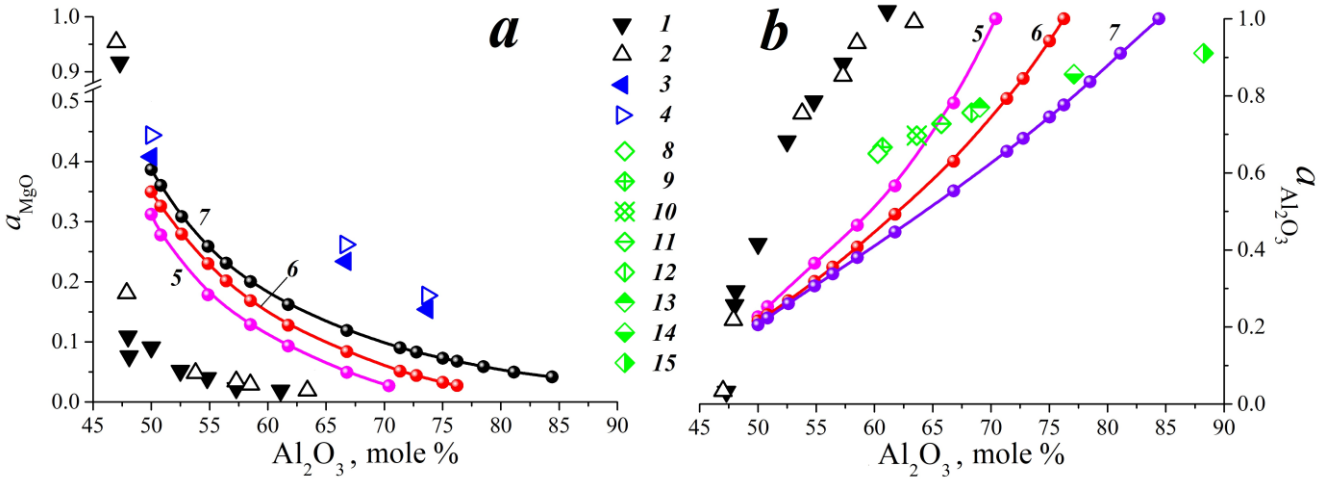

Fig. 3. Activities of MgO (*a*) and Al_2O_3 (*b*) in the spinel solid solutions determined: *1* and *2* – in the heterogeneous equilibrium study at 1800 and 1877 K (Fujii et al., 2000); *3–7* – by the Knudsen effusion mass-spectrometric method at 2073 and 2173 K (Sasamoto et al., 1981), as well as at 2000, 2100 and 2200 K at present study, respectively; *8–15* – calculated by Navrotsky et al. (Navrotsky et al., 1986) at 1723, 1750, 1800, 1850, 1900, 1923, 2073 and 2173 K, respectively.

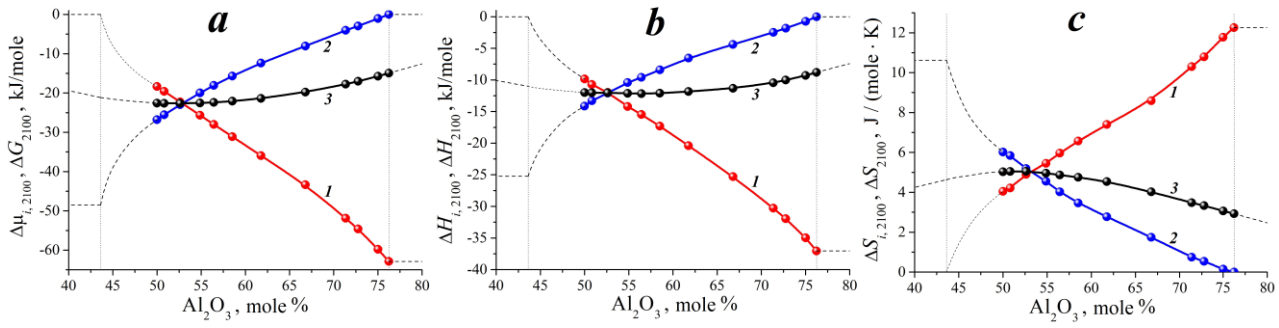

Fig. 4. The oxide chemical potentials and the Gibbs energy (*a*), the oxide partial enthalpies and the enthalpy of melt formation (*b*) and the oxide partial entropies and the entropy of melt formation (*c*) of spinel solid solutions at 2100 K. Table of symbols: *1* – MgO, *2* – Al_2O_3, *3* – integral thermodynamic characteristics (Gibbs energy, enthalpy and entropy of formation of spinel solid solutions, respectively). The vertical dashed lines indicate the boundaries of the spinel solid solutions.

The present study was supported by RAS Presidium's Program #7 (**Experimental and theoretical studies of Solar system objects and star planetary systems**. Transients in astrophysics).

References:

Belton G. R., Fruehan R. J. (1971) The determination of activities of mass spectrometry: some additional methods. *Met. Trans. B*, vol. 2, no. 1, pp. 291–296.

Berezhnoi, A. S. (1970) Multicomponent oxide systems. Kiev: Naukova Dumka, 544 pp.

Glushko V. P., Gurvich L. V., Bergman G. A., Veitz I. V., Medvedev V. A., Khachkuruzov G. A., Yungman V. S. (1978-1982) Thermodynamic properties of individual substances. Moscow: Nauka, vol. 1–4.

Fujii K., Nagasaka T., Hino M. (2000) Activities of the constituents in spinel solid solution and free energies of formation of MgO, MgO · Al_2O_3. *JISJ Intern*., vol. 40, no. 11, pp. 1059–1066.

Komlev G. A. (1964) Determination of the saturated vapor pressure by the effusion method. *Russ. J. Phys. Chem*., vol. 38, no. 11, pp. 2747–2748.

Lewis G. N., Randall M. (1923) Thermodynamics and the free energy of chemical substances. New York: McGraw-Hill, 653 pp.

Navrotsky A., Wechsler B. A., Geisinger K. L., Seifert F. (1986) Thermochemistry of $MgAl_2O_4$–$Al_{8/3}O_4$ defect spinels. *J. Amer. Ceram. Soc*., vol. 69, no. 5, pp. 418–422.

Prigogine I., Defay R. (1954) Chemical thermodynamics. London: Longman, 543 pp.

Ronchi C., Sheindlin M. (2001) Melting point of MgO. *J. Appl. Phys*., vol. 90, no. 7, pp. 3325–3331.

Sasamoto T., Hara H., Sata T. (1981) Mass spectrometric study of the vaporization of magnesium oxide from magnesium aluminate spinel. *Bull. Chem. Soc. Japan*, vol. 54, no. 11, pp. 3327–3333.

Sidorov L. N., Korobov M. V., Zhuravleva L. V. (1985) Mass-spectrometric thermodynamic studies. Moscow: MSU, 208 pp.

Shornikov S. I., Archakov I. Yu., Chemekova T. Yu. (2000) A mass spectrometric study of vaporization and phase equilibria in the Al_2O_3-SiO_2 system. *Russ. J. Phys. Chem*., vol. 74, no. 5, pp. 677–683.

Shornikov S. I. (2002) Thermodynamic study of the mullite solid solution region in the Al_2O_3–SiO_2 system by mass spectrometric techniques. *Geochem. Int*., vol. 40, suppl. 1, pp. S46–S60.

Shornikov S. I. (2015) Vaporization coefficients of oxides contained in the melts of Ca–Al–Inclusions in chondrites. *Geochem. Int*., vol. 53, no. 12, pp. 1080–1089.

Shornikov S. I. (2017a) Mass spectrometric investigation of evaporation processes of $MgAl_2O_4$. *Russ. J. Phys. Chem. A*, vol. 91, no. 1, pp. 10–16.

Shornikov S. I. (2017b) Thermodynamic properties of spinel $MgAl_2O_4$: a mass spectrometric study. *Russ. J. Phys. Chem. A*, vol. 91, no. 2, pp. 287–294.

Wark D., Boynton W. V. (2001) The formation of rims on calcium-aluminum-rich inclusions: step I – Flash heating. *Met. Planet. Sci*., vol. 36, no. 8, pp. 1135–1166.